Lineament Interpretation of the Revell Batholith and Surrounding Greenstone Belts

NWMO-TR-2018-19 December 2018

Aaron DesRoches, Martin Sykes, Andy Parmenter, Eric Sykes

Nuclear Waste Management Organization

nwmo
NUCLEAR WASTE MANAGEMENT ORGANIZATION
SOCIÉTÉ DE GESTION DES DÉCHETS NUCLÉAIRES

Nuclear Waste Management Organization
22 St. Clair Avenue East, 6th Floor
Toronto, Ontario
M4T 2S3
Canada

Tel: 416-934-9814
Web: www.nwmo.ca

Lineament Interpretation of the Revell Batholith and Surrounding Greenstone Belts

NWMO-TR-2018-19

December 2018

Aaron DesRoches, Martin Sykes, Andy Parmenter, Eric Sykes
Nuclear Waste Management Organization

Document History

Title:	Lineament Interpretation of the Revell Batholith and Surrounding Greenstone Belts		
Report Number:	NWMO-TR-2018-19		
Revision:	R000	Date:	December 2018
Nuclear Waste Management Organization			
Authored by:	Aaron DesRoches, Martin Sykes, Andy Parmenter, Eric Sykes		
Reviewed by:	Sarah Hirschorn		
Accepted by:	Sarah Hirschorn		

ABSTRACT

Title: Lineament Interpretation of the Revell Batholith and Surrounding Greenstone Belts
Report No.: NWMO-TR-2018-19
Author(s): Aaron DesRoches, Martin Sykes, Andy Parmenter, Eric Sykes
Company: Nuclear Waste Management Organization
Date: December 2018

Abstract

Performing a structural lineament interpretation is an important component of the assessment of a crystalline bedrock setting, where the interpreted lineaments have the potential to represent the surface expression of faults and fractures that may act as potential groundwater flow pathways, zones of geomechanical instability or potential reactivation. Previous lineament interpretations in the Ignace area were completed at maximum scale of 1:25,000. Since the Revell Site was selected as the area for initial borehole drilling, an updated interpretation of lineaments was completed at a closer scale.

This report documents the specific data sources, workflow, and results from an updated lineament interpretation for the Revell Batholith and surrounding greenstone belt areas. The lineament interpretation is based on high-resolution remote sensing data sets, including a high-resolution airborne magnetic data, high-resolution surface topographic data and digital orthoimagery data collected during the airborne LIDAR survey. The updated lineament analysis provides an interpretation of the location and orientation of possible brittle and dyke lineaments, as well as fabric-concordant lineaments interpreted within the greenstone belt units.

Within the Revell Batholith and surrounding greenstone belt area, a total of 192 magnetic lineaments, and 4676 surficial lineaments were interpreted to from their respective data sets. The integration of magnetic and surficial lineaments for the Revell Batholith area resulted in a total of 4701 lineament traces. As a result, the integrated lineaments comprise 3668 lineaments interpreted as brittle structures, 1023 lineaments interpreted as fabric-concordant structures, and 10 lineaments that are interpreted as diabase dykes.

The integrated lineament data set results represent a combined analysis of the magnetic and surficial lineaments, and are believed to reflect the most accurate lineament traces from the source data. Lineament coincidence analysis resulted in a total of 113 (2.4%) lineaments that were observed in both the magnetic and the surficial data sets. The lack of coincidence between magnetic and surficial lineaments could be attributed to multiple variables, including features identified in the surficial data may not possess sufficient magnetic susceptibility contrast to be recognized in the magnetic data, and masking of surface expressions of magnetic lineaments by the presence of overburden.

Evaluating lineament lengths of the final integrated lineaments resulted in lengths ranging from 17 to 13470 m, with a median length of 193 m and mean length of 402 m. Statistical descriptors were calculated that describe the fit of the lineament lengths to both lognormal and power law distributions. Although lineament lengths fit well to the lognormal distribution, calculated skewness coefficients suggest the data has a slight positive skew. In addition, cumulative frequency of lineament lengths fit the power law curve over the portion of data where measured lengths are not influenced by sampling bias effects, however deviate from the curve as a result of censoring and truncation.

Azimuth analysis of the entire integrated lineament data set, including all 4701 inferred structure types (brittle, fabric-concordant and dyke), are subdivided into a NE trending peak with a mean azimuth of 38° and a SE trending peak with a mean azimuth of 130°. The fabric-concordant lineaments display a pronounced SE trend, comprising of 649 lineaments with a mean azimuth of 127° and also display two subordinate sets; N and NE trends as a result of these lineaments following the variation in the ductile fabric around the northwestern edge of the Revell Batholith. Results suggest that the spatial distribution of fabric-concordant lineaments could be subdivided into three structural domains and characterized by unique azimuth statistics. Ten dyke lineaments show fairly consistent trends resulting in a mean azimuth of 110°. Alternatively, these dyke lineaments could be subdivided into two discrete sets with peaks at 101° and 119°, separated by a small angle, where the peak trending 101° tends to comprise short en-echelon segments linking the longer dykes that comprise the peak trending 119°. Within the Revell Batholith, five 5 well-defined brittle lineament trends (N, NE, ENE, ESE, SE) are identified when analyzing lineaments with lengths greater than 500 m.

Overall, the process of interpreting lineaments from remotely sensed data inherently has varying degrees of uncertainty. Uncertainty can be associated with location accuracy of a given lineament trace, which can depend on the discreteness and continuity of the feature identified in a source data set. Uncertainty may be associated with the nature and extent of overburden coverage that may mask the bedrock surface, resulting in poor lineament identification from surficial datasets. Also, uncertainty may also be associated with a poor magnetic contrast between the rock mass and potential fracture zones, which can limit the interpretation of lineaments from airborne magnetic survey data. Ultimately, the greatest uncertainty is whether the interpreted lineaments actually represent the surface expression of structures that project into the subsurface, or whether or not they are hydraulically conductive. Ultimately, these uncertainties and others should be managed through additional surface geological mapping and borehole drilling, where specific lineaments can be further characterized and their uncertainties reduced.

Results from this updated structural lineament interpretation will contribute towards a further understanding of the structural framework of the Revell Batholith and surrounding greenstone belt area. As such, the resulting lineament data sets will provide the initial framework for construction of multiple discrete fracture networks (DFN), and subsequently form the input in to groundwater flow scenarios for the area.

TABLE OF CONTENTS

LIST OF TABLES

Page

LIST OF FIGURES

Page

1. INTRODUCTION

This technical report documents the methodology and results from an updated structural lineament interpretation completed for a portion of the Revell Batholith and surrounding greenstone belt units near the communities of Wabigoon Lake Ojibway Nation and Ignace, Ontario.

During NWMO Phase 1 Desktop Assessments, a regional-scale lineament investigation was completed, which relied on the use of publically available geophysical and remote sensing data (JDMA 2011). As a part of NWMO Phase 2 field investigations a high-resolution airborne magnetic data set (SGL, 2015) was acquired and subsequently used to update the lineament interpretation for the region near the community of Ignace, Ontario (SRK 2015). In the fall of 2017, NWMO contracted ATLIS Geomatics to acquire a high-resolution LiDAR and orthoimagery data set for part of the Revell Batholith and surrounding greenstone belt. The use of this high-resolution data set allowed for a more focused lineament interpretation to be completed for this area, resulting in the third lineament interpretation completed. This focused lineament interpretation will supersede both the previous regional scale interpretation completed by JDMA (2011) and SRK (2015). A high-resolution lineament interpretation was completed over a region of the Revell Batholith and surrounding greenstone units by combining high-resolution airborne magnetic, LiDAR and orthoimagery data sets.

1.1 Purpose

The purpose of updating the structural lineament interpretation for the Revell Batholith area was to:

a) Develop a new structural lineament interpretation that specifically focuses on an area that was selected as being potentially suitable for hosting a deep geological repository;
b) Update the structural framework for the potential siting area in the Revell Batholith area that was identified as part of Phase 2 Site investigations; and
c) Provide structural lineament information that will be utilized to generate discrete fracture network (DFN) realizations for the Revell Batholith area, forming valuable input in the ongoing planning for borehole drilling, future groundwater flow simulations and the overall geosphere conceptual model.

The results from the structural lineament interpretation will be used to identify specific areas for future detailed geological mapping, and drilling within the study area. Lineament traces, and the analysis of their linear attributes will be used to support the development of multiple Discrete Fracture Network (DFN) model simulations for the area.

1.2 Location

The current updated structural lineament interpretation was completed for a portion of the Revell Batholith and surrounding greenstone belt units between the communities of Wabigoon Lake Ojibway Nation and the Township of Ignace in Northwestern Ontario. The lineament interpretation extent is 495 km^2 and is located approximately 22 km from the Wabigoon Lake Ojibway Nation boundary, and 35 km from the Township of Ignace boundary to the centroid of the interpretation extent (Figure 1).

Overall, the geometry of the Revell Batholith is roughly elliptical in shape. It trends northwest and is approximately 40 km in length, 15 km in width, and covers an area of approximately 455 km^2. Different intrusive granitoid phases have been recognized within the batholith (Stone et al., 2011a and 2011b), which is surrounded by the Raleigh Lake (to the north and east) and Bending Lake (to the southwest) greenstone belts. The Raleigh Lake greenstone belt is dominated by mafic metavolcanic rocks, and contains approximately 30% intermediate to felsic fragmental metavolcanic rocks (Stone, 2010a). The greenstone belt is intruded by small oval felsic to intermediate plutons such as the Raleigh Lake intrusion. The Bending Lake greenstone belt is composed of mafic metavolcanic rocks, with subordinate gabbro, intermediate metavolcanic rocks, and clastic metasedimentary rocks (wacke and argillite; Stone, 2010b).

See Golder (2013) and Golder and PGW (2017) for detailed descriptions of the Revell Batholith and surrounding greenstone belt bedrock geology.

2. METHODOLOGY

2.1 Source Data and Processing

Data sets used for structural lineament interpretation consist of high-resolution airborne magnetic data (SGL, 2015), and newly acquired high-resolution LiDAR and Orthoimagery data sets acquired by ATLIS in the Fall of 2017 (ATLIS 2018).

Various grid and raster enhancements have been applied to each of these data sets in order to highlight subtle details not evident in the base source data. The following subsections describe each of the data sets and the enhancements applied.

2.1.1 Airborne Magnetic Data

The following data sets, calculated by Sander Geophysics Ltd (SGL 2015), were used for the interpretation of lineaments within the Revell Batholith and surrounding greenstone belt area. The magnetic data were acquired along 100 m traverse lines, and 500 m perpendicular controls lines at a target altitude of 80 m above ground surface. However, this data only covers approximate 70% of the lineament interpretation footprint (i.e. does not cover the western portion of the area). The acquired data were interpolated between flight lines and control lines using a 25 m grid cell. For airborne magnetic surveys this is considered to be a high-resolution data set. The remaining footprint not covered by the SGL survey is located over the metavolcanic and metasedimentary units of the greenstone belt to the west of the Revell Batholith. For this remaining area, airborne magnetic data gathered and processed during the NWMO Phase 1 study (PGW 2013, OGS 2011a) was used to supplement the western portion of the lineament interpretation extent, which includes data acquired along 200 m traverse lines, and 800 m perpendicular controls lines at a nominal altitude of 73 m above ground surface.

Using the acquired magnetic data the following enhanced data sets were used for the lineament interpretation:

- Reduced to pole transformation of total magnetic field
- First vertical derivative of reduced to pole total magnetic field (Figure 3)
- Second vertical derivative of reduced to pole total magnetic field
- Horizontal gradient of total magnetic field
- Analytic Signal of total magnetic field
- Tilt Angle product of reduced to pole total magnetic field.

2.1.2 Digital Elevation Model

The digital elevation model (DEM) data were acquired during a LiDAR survey completed by ATLIS in the Fall of 2017 (ATLIS 2018). LiDAR data was acquired using a Leica ALS70-HP sensor with a field of view of 40 degrees and a side lap of 50% in order to obtain a minimum spatial data point density of 8 p/m^2. The survey was flown at an altitude of 1500 m and has a final vertical accuracy of <15cm at 95% confidence. The LiDAR data were processed by ATLIS to obtain a DEM of the ground surface (trees removed) with a final cell size of 1 m, which was used for the lineament interpretation. Using the DEM provided by ATLIS the following grid enhancements were performed to emphasize lineaments within the data:

2.1.2.1 Analytic Hill Shading

Hill shading was performed on the DEM data set using three separate azimuth directions (i.e. 45, 270, and 360 degrees), using a uniform declinations (45 degrees), and a vertical exaggeration of 2. Linear river valleys and terrain slopes are emphasized by the hill shading process, allowing for the linear features to be manually traced. The analytic hill shading was computed using QGIS.

2.1.2.2 Convergence Index

The convergence index (CI) was used to define areas of converging topography. The calculation is based on the slope aspect (as described by Thommeret et al 2009) performed within a specified circular moving window with a 10 m cell radius, where convergence represents the average angular value between each of the neighboring cells and the center cell in the moving window. The resulting convergence index values range from -90 to 90 degrees. Within the resulting grid, positive values represent areas of divergence, and negative values represent areas of convergence. Null or zero values represent flat areas. The convergence index was computed using QGIS.

2.1.2.3 Residual Analysis

Using the DEM surface derived from the LiDAR data a number of residual grids were calculated based on neighbouring cells within a 10 m circular radius. Cell values that fell within the circular radius were used to calculate the mean cell value, difference from the mean value, standard deviation, range of values, maximum and minimum values, deviation from the mean value, and percentile values. The difference from mean value and deviation from mean value are similar to high-pass filters and emphasize linear river valleys and steep slopes. The other grids were used to define other morphological characteristics.

2.1.2.4 Terrain openness

The terrain openness map (Figure 4) is a terrain morphology metric that can be used to visualize the terrain by combining positive and negative openness characteristics extracted from the digital elevation data (Yokoyama, 2002). The terrain openness is the angle between surface relief and the horizontal distance, characterized as the maximum upward or downward angle over a specific search window. The specified search window was defined with a radial limit of 1000 m. In contrast to conventional shading methods, this has the advantage of being independent of the direction of the light source.

2.1.3 Orthoimagery

Orthoimagery was simultaneously acquired during the LiDAR survey by ATLIS in the Fall of 2017. Orthoimagery data were acquired using a Leica RCD30 4-band sensor to capture the

images in true colour with an overall cell size of 15 cm. Using the provided Orthoimagery with differentiated red, blue, green and near infrared colours (RGB+NIR), minor data enhancements applied are described below.

2.1.3.1 Colour Composites

For visual analysis, color composites make full use of the capabilities of the human eye. Colour composite generation involves selecting the specific wavelength bands to combine and associated contrast and colour stretching. Bands 3, 2, 1 represent the true colour image of the area (Figure 5). A composite of bands 4, 3, 2 include the near infrared wavelength, and can be used to increase the contrast between vegetation, water and bedrock.

2.1.3.2 Edge detection filters

Edge detection filters were applied to imagery data, such as the Sobel and Prewitt filters to detect boundaries or changes in image texture. The Sobel method consists of two 3x3 moving windows in the horizontal and vertical direction, which can also be modified to detect edges in the positive and negative diagonal directions, whereby each is implemented separately and then combined to obtain the optimal edges. The Prewitt filter is similar to the Sobel filter in that it has the same window size, design and zero center weight, except it uses negative and positive ones in place of twos. These filters were used for emphasizing locations of bedrock, rivers and streams, vegetation, etc.

2.2 Lineament Interpretation Workflow

Using the data sets described in Section 2.1, a structural lineament interpretation of the Revell Batholith area was completed to identify locations and orientations of potential faults and/or fracture zones. The data sets described in Section 2.1 were compiled in QGIS 2.18.3 (QGIS 2017).

The lineament interpretation of the Revell area was performed jointly by two NWMO subject matter experts (SMEs) using a rigorous workflow and was completed as part of an updated collaborative lineament interpretation. The purpose of this updated collaborative lineament interpretation workflow was to have the SMEs agree on the precise geometry, and characteristics of each lineament trace during the interpretation process. Previous lineament interpretation workflows included having two SMEs interpret lineaments independently, and then integrating their lineament traces together to generate a final lineament interpretation (SRK 2015). Although that workflow helped to minimize subjectivity of individual lineaments by having two sets of independent interpretations, the process of integrating two lineament data sets together introduced some digitization error in the interpretation caused by manually selecting and merging lineaments. The new updated workflow is designed to minimize the amount of post-interpretation merging of lineaments, build consensus between the two SME interpreters, while reducing the uncertainty in the interpretation due to subjectivity.

The lineament interpretation included the documentation of a detailed attribute table capturing important characteristics that describe each interpreted feature (Table 1). Following the completion of each interpreted lineament data set, they were reviewed by a team of two additional NWMO SMEs to confirm the accuracy of lineament attributes recorded, and accuracy of lineament geometries based on their original source data sets.

Table 1: Summary of Attribute Table Fields to be populated for the Lineament Interpretation

ID	Attribute	Brief Description
1	Int_ID	Interpreter identification - Initials for each interpreter
2	Rev_ID	Reviewer identification - initials for each reviewer
3	Feat_ID	Feature identification - Unique numeric lineament feature identifier (123, 324, 435, etc)
4	Data_typ	Data type - Data set used (MAG, LiDAR)

5	Certainty	Value describing the confidence in the feature being related to bedrock structure (1-low, 2-medium or 3-high).
6	Length	Length of feature is the sum of individual lengths of mapped polylines and is expressed in kilometers
7	Length_Cur	Curvature metric of the length field (ratio of the start to end length and the sum of polyline segment length
8	Azimuth	Lineament orientation expressed as clockwise degree rotation from north (from 0 to 180)
9	Buffer_LCA	Buffer zone width for lineament coincidence assessment
10	LCA	Feature value (1, or 2) based on lineament coincidence assessment (LCA)
11	MAG	Feature identified in magnetic (MAG) data set (Yes or No)
12	SURF	Feature identified in surficial (SURF = DEM and Orthoimagery) data set (Yes or No)
13	Notes	Comment field for additional relevant information on a feature
14	Inferred	Geological element identified, e.g., brittle, dyke, fabric-concordant

2.2.1 Lineament Tracing

The systematic workflow for tracing lineaments involved subdividing the lineament interpretation extent into square tiles of equal area shown in Figure 6. In this case, the interpretation extent can be separated into 31 tiles each with a 25 square km area (i.e. 5 x 5 km tiles). Tracing of lineaments occurred within the extent of a single tile portion and, as needed, the trace line extended into neighbouring tiles to capture the full length. Once the interpretation of a single tile was complete the interpretation of the neighbouring tile was initiated.

Lineaments were traced at all possible scales, as dictated by the resolution of the data sets being used, and the scale at which lineaments were observed within the extent. At this stage, all interpreted lineaments were traced as accurately as possible from the data set.

Also, it is acknowledged that linear features traced near the edge of the survey extent may continue beyond the boundary of the lineament interpretation footprint (red outline in Figure 1), however, their lineament trace was terminated at the boundary. In these cases, the trace length of these lineaments will not represent the maximum trace length due to truncation at the boundary.

To understand the large-scale structural context within the study area, lineaments were first interpreted using the airborne magnetic data set and enhanced magnetic derivative grids, followed by an interpretation of the surficial remote sensing data sets (LiDAR DEM and Orthoimagery). Interpretation of the magnetic data sets (Section 3.1) involved tracing well-defined discontinuities in form lines, offset of magnetic units, or the presence of linear magnetic lows or highs interpreted faults, fracture zones and mafic dykes. Fault and fracture zones are often interpreted as well-defined linear features traced along discrete lows in magnetic field data resulting from the alteration of common magnetic minerals (e.g. magnetite) in the bedrock. However, because the tonalite, granite and granodiorite bedrock of the Revell Batholith are broadly characterized by a low background magnetic susceptibility, the appearance of fault and fracture zones is often suppressed in the magnetic data set. In addition, because the Revell Batholith is adjacent to the Bending Lake and Raleigh Lake Greenstone belts, it is suspected that eroded magnetite-rich sediments have been transported and deposited along lakes, streams and river valleys in the batholith resulting in a slightly elevated magnetic field response along these lineaments relative to the background magnetic field in which case some lineaments with an inferred brittle nature have been traced along continuous magnetic highs.. The presence of known diabase dykes within the study area are well defined by high magnetic total field responses. These linear features can be traced with a high-degree of accuracy and confidence due to the presence of a high magnetic susceptibility contrast between the diabase dykes and the Revell Batholith bedrock, in particular in the higher order magnetic derivative grids.

After completing the magnetic lineament interpretation, lineaments were interpreted concurrently using the LiDAR DEM and Digital Aerial Orthoimagery data to generate a network of surficial lineaments. Both data sets present the same high-resolution surficial expression of lineament features, and provide excellent mutually supporting data sets. The lineament interpretation involved tracing lineaments along topographic valleys, escarpments and breaks in

slope, and any other structurally related topographic features that are visible the enhanced DEM products listed in Section 3.2. In addition, the lineament interpretation of digital aerial orthoimagery involved drawing lineaments along straight segments of shore lines, changes in colour intensity or texture (e.g., vegetation), rivers and streams and along linear chains of features associated with lakes.

Outputs from this lineament tracing stage of the interpretation resulted in two independent lineament shapefiles; magnetic lineament and surficial lineament data sets, and the characteristics for individual lineaments were populated in the attribute table.

2.2.2 Lineament Integration and Coincidence

An important characteristics of an individual lineament trace is whether it occurs within multiple data sets. This is a manual process involving expert judgement and the combined visualization of both lineament interpretations to determine if the traces coincide with the same bedrock structure. Relying on a systematic workflow, the two lineament data sets were evaluated within the same 5 x 5 km tile index (31 tiles) used during the preceding trace interpretation stage. Any lineament that only occurred in a single data set was copied to the integrated lineament data set and assigned an LCA value of 1 (e.g. meaning this lineament is only observed in a single data set). All remaining lineaments, where some portion of their traces overlap, were evaluated by both SMEs to determine their coincidence and reconcile their trace geometries. Reconciling trace geometry often required some form of manual trace modifications (e.g. merging of lineament traces in the overlapping region) and relied on the use of appropriate high-resolution grid data sets to guide the decision. The integration data resulted in the most accurate lineament traces that reflect the source data.

Differences in interpretation scale and resolution of data sets can lead to problems with determining lineaments that are coincident. In some cases, differences in grid cell resolution between airborne magnetic and the LiDAR and orthoimagery data sets results in a disagreement between the interpreted trace location between data sets. For example, linear features interpreted from the airborne magnetic data tend to be distinguished by larger wavelengths anomalies, compared to lineaments interpreted from the surficial data sets (LiDAR and Orthoimagery), whereby the geospatial position of the lineament trace tends to be less certain. Since lineaments from LiDAR and orthoimagery data sets are well resolved geospatially, these lineaments tend to be more reliable and are used primarily in the integration process to represent the accurate trace location coinciding with a possible underlying brittle structure.

As a guide for lineament trace modifications, an additional raster grid was developed to aid the identification of coincidence between lineaments from the two lineament data sets. The raster was calculated by converting each polyline to polygons that have widths equal to a defined buffer. The buffer width was determined subjectively based on the resolution of the data sets used, and the width of the traced features. Lineament polygons from the two data set were converted to binary raster images, where lineaments were assigned a raster value of one, and the remaining areas were set to zero. Using a raster calculator, the two binary rasters were summed to show where lineaments either cross-cut, or are coincident.

2.2.3 Lineament Azimuth

Calculating the azimuth of lineament traces is important for determining whether interpreted brittle structures have consistent patterns with well-defined trends, or whether there is a complex network of structures. There are several different approaches for calculating azimuth of a polyline features in GIS softwares (e.g. end to end azimuth, center point to end azimuth). However, because the interpreted lineament traces are made up of multiple polyline segments

with varying lengths, a segment length-weighted approach was developed to derive the mean azimuth of each lineament. This approach accounts for azimuthal variability of each polyline segment on the overall lineament azimuth. The calculation was performed using a batch processing modeller module in QGIS to sequentially perform various attribute calculations. Pre-processing of each lineament was required to perform the azimuth calculation, which included subdividing each lineament trace into individual polyline segments consisting of a single line connecting two end nodes. Each polyline segment retained its unique lineament identifier, which following the calculations, was used to recombine the segments to their original lineament traces. For each segment, node to node length and azimuth were calculated. This data is then used to calculate the length-weighted mean for each set of segments that comprise the initial lineament trace (i.e. based on the unique lineament identifier). These calculations rely on circular azimuth statistical methods (Mardia, 1972), which take into account azimuth values crossing over from 359 to 0 degrees (i.e. a simple mean would result in erroneous values). Figure 7 shows a schematic of a lineament trace comprising four polyline segments and 5 nodes. In the calculation of mean azimuth, each polyline segment is characterized by its individual length and azimuth from its start and end nodes. The schematic shows two longer polylines with similar azimuths, and two short polylines with varying azimuths, where the length of the polylines determine the amount of influence individual polyline azimuths have on the assigned mean azimuth. This approach to calculating azimuth provides a more accurate azimuth value compared to simply calculating azimuth between two polyline endpoints.

Mean lineament azimuths were evaluated using rose diagram plots to depict dominant trends in orientation (azimuthal) data and the relative frequency for each bin. Rose diagrams were produced in Spheristat (v. 3.2.1), with frequencies divided into 5° bins in order to avoid oversimplification of the lineament orientations. The calculated lineament lengths are also used as a weighting factor to highlight orientations that are dominated by longer lineaments.

Dominant lineament trends or peaks are defined in Spheristat. In order to define peaks that are statistically meaningful, the peaks were defined by plotting the expected frequency for a uniform, isotropic distribution of the number of data being analysed. The 95% confidence level is calculated to be twice the standard deviation (E) of the distribution. Spheristat plots these levels as dashed circles above and below E, if they occur in the frequency range selected. Where the plotted azimuth data on the rose diagram shows a discrete peak which exceeds the expected uniform distribution, it is defined as a representative azimuth trend and a dominant azimuth can be defined.

2.2.4 Lineament Length

Lineament trace length can be used as a proxy for understanding the extent of bedrock deformation (i.e. longer lineaments may extend to greater depths). Lineament lengths were calculated as the sum of line segments that make up the lineament trace.

A curvature metric is also calculated for each lineament by taking the ratio of the start to end length by the sum of polyline segment length, providing a value ranging from 0 to 1. The highest values represent lineaments with very little curvature. Higher degrees of curvature are indicated by values <1, with a value of 0 having the highest degree of curvature. This metric can be used to identify lineaments that have more curvature, whereby their azimuth varies significantly along their length (e.g. curved lineaments concordant with ductile fabric of greenstone units).

2.2.5 Lineament Type based on Geological Interpretation

Following the integration stage lineaments were subdivided into separate types based on an interpretation of available geological information. Inference of lineament type was primarily based on structural evidence from previous local- and regional-scale mapping completed in the Revell Batholith, and adjacent greenstone belt units (Satterly, 1960, Kresz et al 1982, Stone et al 2011a, Stone et al 2011b), in addition to textural and amplitude responses from magnetic and

enhanced derivative grids, and LiDAR derived topographic data. Within the metavolcanic and metasedimentary units of the greenstone belts, trends of planar ductile features (e.g. foliation, schistosity, bedding, gneissosity, etc) from local- and regional-scale mapping were used to inform the interpretation.

Where lineament traces were shown to be concordant to the planar ductile fabric within the greenstone belts, these lineaments were classified as fabric-concordant lineaments. Fabric-concordant lineaments are characterized by semi-continuous linear to curvi-linear features in either the topographic or magnetic data, which may represent a wide range of structures including metavolcanic and metasedimentary layering, tectonic foliation, schistosity or gneissosity, ductile shear zones (i.e. intensification of foliation across a narrow zone) or brittle-ductile shear zones (i.e. intensification of foliation across a narrow zone with associated fracturing), or possible brittle structures reactivated along the planar ductile fabric. Additional field investigations are required to determine the true nature of these lineaments. However, as a conservative approach, these lineaments may be represented as being hydraulically conductive in groundwater flow simulations, but an important consideration is that their geometries are generally well-understood as being concordant with the orientations of planar ductile features from mapping (i.e., foliation, schistosity, bedding, gneissosity, etc).

Lineaments within the greenstone belt that cross-cut the planar ductile fabric, and the majority of lineaments traced within the Revell batholith are inferred to be brittle lineaments. In general, brittle lineaments within the greenstone belt are assumed to post-date the fabric-concordant lineaments, such that their trace cross-cuts the planar ductile fabric. However, this relative age relationship may not always be the case if any ductile fabric has undergone a period of late brittle reactivation. In either the greenstone belt or the batholith, the brittle lineaments tends to be characterized by linear to curvi-linear traces in the magnetic or topographic data sets, which are interpreted as potential zones of increased fracturing (e.g., joints or joint sets, faults or fault zones, and veins or vein sets). Within the magnetic data, these brittle lineaments are manifested as linear magnetic lows, associated with a contrast in magnetic susceptibility with the bedrock. In the LiDAR and Orthoimagery data, these brittle lineaments are manifested as clear linear discontinuities in topography and vegetation and are often associated with rivers and streams.

Lastly, dyke lineaments were inferred within the lineament investigation area primarily based on very distinct high linear magnetic anomalies through both the Revell Batholith and adjacent greenstone units. These linear magnetic anomalies are continuous, and extend through the entire investigation area. Although these dyke lineaments are also locally represented in the LiDAR topographic data, their inference as dykes is solely based on the magnetic data. Since these lineaments have been well-mapped on surface (Satterly, 1960, Stone et al 2011a, Stone et al 2011b), and their response is distinct in the magnetic data, their interpretation as a diabase dyke can be assigned with a high degree of certainty.

3. RESULTS

The following sections describe the results of the lineament interpretation of the Revell Batholith area based on analysis of the airborne magnetic and surficial (LiDAR, Orthoimagery) data sets. This includes description of results for the integration and coincidence assessment between these data sets.

3.1 Magnetic Lineaments

Within the Revell Batholith and surrounding greenstone belt area, a total of 192 lineaments were interpreted from the magnetic data (Figure 8). This included interpretation of 100 features characterized by discrete linear magnetic lows and interpreted as brittle lineaments (e.g., Figures 9A and 9B), 82 features concordant with the trend of the ductile fabric within the greenstone units and interpreted as fabric-concordant features (e.g., Figure 9C) and 10 features characterized by discrete linear magnetic highs corresponding to interpreted dyke lineaments (e.g., Figure 9D).

The length of all magnetic lineaments ranges from 275 to 12763 m, with a median of 1998 m and a mean of 2620 m. The descriptive statistics for magnetic lineament lengths are presented in Table 2.

Table 2: Descriptive statistics for magnetic lineament lengths

Magnetic Lineaments	Length [m]
Number of values	192
Minimum	275
Maximum	12763
Mean	2620
Median	1998
First quartile	1200
Third quartile	3379
Standard deviation	1999

The 100 interpreted brittle lineaments primarily occur within the main body of the Revell Batholith; only 5 of the brittle lineaments were interpreted within the surrounding greenstone belt. In the latter case, brittle lineaments were identified by their discordance to the dominant ductile fabric trend. The majority of brittle lineaments are present in the southeastern part of the Revell Batholith, within a megacrystic phase, characterized by a positive magnetic anomaly associated with rocks with higher magnetic susceptibility, although brittle lineaments are also present throughout the rest of the batholith.

The 82 interpreted fabric-concordant lineaments tend to be concordant to the regional ductile fabric mapped in the greenstone belt, and are interpreted to represent potential structural discontinuities or primary layering along the metavolcanic to metasedimentary units. Such discontinuities may represent potential fractures or fracture zones or faults. Figure 9C displays mapped ductile foliation striking parallel to the dominant trend of the fabric-concordant magnetic anomalies.

The 10 interpreted dyke lineaments occur within a relatively narrow band (approx. 3 km wide) trending northwesterly through the central portion of the batholith. These lineaments are well

characterized by their high magnetic response as a result of a strong magnetic susceptibility contrast with the surrounding bedrock. Consequently, they are traced with high confidence.

3.2 Surficial Lineaments

Interpretation of the LiDAR and orthoimagery data resulted in 4676 lineaments from within the Revell Batholith and surrounding greenstone belt area (Figure 10). At this stage, there was no inference on the lineament type, and all lineaments were considered undifferentiated, as the surficial lineaments were interpreted based solely upon remote sensing data.

In general, lineaments interpreted from the LiDAR and orthoimagery data are shorter than those interpreted from the magnetic data due to the distribution of surface cover (e.g. overburden and water features). The lengths of all surficial lineaments range from 17 to 13470 m, with a median of 189 m and a mean of 331m. The descriptive statistics for surficial lineament lengths are presented in Table 3.

Table 3. Descriptive statistics for surficial lineament lengths

Surficial Lineaments	Length [m]
Number of values	4676
Minimum	17
Maximum	13470
Mean	331
Median	189
First quartile	110
Third quartile	350
Standard deviation	574

In general, the spatial distribution of interpreted surficial lineaments is influenced by the distribution of exposed bedrock, such that locations where bedrock is covered by either glacial overburden or water features, the density of lineaments is low (see Figure 11). As a way to visualize this influence, an airborne electromagnetic data set, previously flown by the Ontario Geological Survey (OGS 2011a), was used to highlight areas that are inferred to be covered by overburden or water features. By taking advantage of the high electrical conductance contrast between typical resistive granitoid bedrock and conductive overburden and water cover, an electromagnetic conductance map with a threshold filter to isolate anomalies greater than 60S (Siemens) was used as a proxy to show areas of higher potential for bedrock to be covered. The use of 60S threshold was chosen because its spatial distribution coincided well with observable overburden and water cover from the LiDAR and orthoimagery data. The filtered conductance map, shown in Figure 11, shows the majority of inferred overburden is located in the north to northwestern portion of the lineament interpretation extent. This area also coincides with a relatively low number of interpreted surficial lineaments.

Figure 12 shows common expressions of surficial morphology interpreted as structural features within the LiDAR source data. Figure 12A shows well-defined narrow and linear topographic valleys within the Revell Batholith interpreted to be structural features. In contrast, Figure 12B, from within the portion of greenstone belt located SW of the Revell Batholith, shows a set of tightly spaced, NW trending linear to curvilinear valleys and escarpments. Much like the fabric-concordant lineaments interpreted from the magnetic data set, these surficial lineaments are concordant with the trend of foliation mapped in the greenstone belt units (e.g. Satterly, 1960,

Stone et al 2011a, Stone et al 2011b). Throughout much of the lineament interpretation area several short and discontinuous, and predominantly NE trending linear valleys are observed, as shown in Figure 12C. These lineaments are predominantly located within the batholith and only where bedrock is well exposed. Although it is believed these short NE trending lineaments are glacial bedrock landforms (i.e. rôche moutonnée), they commonly parallel a NE-trending joint set (Golder and PGW, 2017). Therefore, they have not been excluded from the lineament analysis at this time but may be excluded on a case by case basis following field investigations. Lastly, Figure 12D shows a large area in the northern portion of the lineament interpretation extent that coincides with significant overburden and water feature cover (e.g. wetlands, lakes, meandering rivers, etc). Topographic relief, associated with the river and stream boundaries, and locally with small rock ridges, is minimal and consequently relatively few lineaments are interpreted here.

3.3 Integrated Lineaments

The integration of magnetic and surficial lineaments for the Revell Batholith area resulted in a total of 4701 lineament traces. Following the integration process, lineaments were inferred to be one of three different structure types based on information from this lineament analysis, and other supporting geological mapping information available in the area (i.e. brittle, fabric-concordant, dyke). As a result the integrated lineaments comprise 3668 lineaments interpreted as brittle structures, 1023 lineaments interpreted as fabric-concordant structures, and 10 lineaments that are interpreted as diabase dykes (Figure 13).

When considering all the integrated lineaments their lengths range from 17 to 13470 m, with a median length of 193 m and mean length of 402 m (Table 4). However, these integrated lineaments can now be subdivided based on inferred lineament type. Descriptive length statistics for each inferred lineament type can be viewed in Table 4.

A more detailed evaluation of the integrated lineaments can be found throughout Section 4.

Table 4. Descriptive statistics for integrated lineament lengths

	All Lineaments (Length [m])	Brittle Lineaments (Length [m])	Fabric-concordant Lineaments (Length [m])	Dyke Lineaments (Length [m])
Number of values	4701	3668	1023	10
Minimum	17	17	32	1371
Maximum	13470	13470	7946	13007
Mean	402	349	552	4190
Median	193	172	263	2324
First quartile	110	100	156	1495
Third quartile	369	325	525	7209
Standard deviation	790	703	894	3842

4. DISCUSSION

The following discussion is based on the analysis of the integrated lineament data set.

4.1 Length

Figure 14 shows the distribution of integrated lineament lengths over the entire Revell Batholith and surrounding greenstone unit area for (A) all integrated lineaments and (B) brittle and dyke lineaments. In this report the lineament length distribution is described by a lognormal distribution. Figure 14A shows the lognormal distribution model fit to the data using all 4701 measured lengths, and has a location parameter of 2.33 and a shape parameter of 0.42. The data is characterized by a skewness coefficient of 0.79 and a kurtosis of 0.9. Overall goodness of fit value of 34.1, and a P-value less than 0.0001. Results provide a logarithmic mean of the length distribution at 2.33, which equate to a log distribution descriptor of approx. 214 m, and a logarithmic standard deviation at 0.42. This value is thought to be a better statistical descriptor of the highly skewed length distribution, and differs from the normal arithmetic mean of the length values of approx. 402 m.

Similarly, Figure 14B shows a lognormal distribution model fit to the data using 3679 measured lengths from only the brittle and dyke lineaments. The lognormal fit is described by a location parameter of 2.29 and a shape parameter of 0.41. The data is characterized by a skewness coefficient of 0.84 and a kurtosis of 1.1. Overall goodness of fit value of 26.4, and a P-value of 0.0001. Results provide a logarithmic mean of the length distribution at 2.29, which equate to a log distribution descriptor of approx. 195 m. This value is thought to be a better statistical descriptor of the highly skewed normal length distribution, and differs from the normal arithmetic mean of the length values of approx. 360 m. Although both data sets fit well to the lognormal distribution (Figure 14A and Figure 14B), calculated skewness coefficients suggest the data has a slight positive skew.

Figure 15 shows log-log plots of the normalized cumulative frequency of lineament lengths for (A) all integrated lineaments and (B) brittle integrated lineaments. The cumulative frequency plots were produced using equal size 10 m interval bin values. These plots represent the number of lineaments that have a length exceeding a given value. Data in the plots can be approximated by fitting a power law curve over the portion of data where measured lengths are not influenced by sampling bias effects, such as censoring and truncation (e.g. Pickering et al, 1995). Because the interpretation of lineaments is limited to the area within the interpretation boundary, lineaments that would have extended beyond this boundary are considered to be undersampled (censored) in the data set. This sampling bias predominantly influences longer lineaments such that there is an inflection in the normalized cumulative length distribution. Alternatively, due to the limitation of the interpretation methodology and/or data set resolution, lineaments that cannot be well resolved in the data set are considered to be truncated. This sampling bias appears as a reduced number of shorter lineaments. The power law fit to the data can then be used in discrete fracture simulations to approximate the length distributions over a given domain using the power law exponent (Bour and Davy, 1997).

Based on data in Figure 15 for both (A) all integrated lineaments and (B) brittle integrated lineaments, censoring starts to occur at lengths of approximately 200 m where the number of lineaments shorter than 200 m decrease and the data points deviate from the power law curve. This length represents the practical lower limit that could be interpreted using the GIS based lineament interpretation method described in Section 2. Truncation starts to occur at lineament lengths greater than approximately 2000 m. Fitting the power law curve over the portion of data where measured lengths are not influenced by censoring and truncation results in an exponent of -1.21 for all the integrated lineaments, and an exponent of -1.28 when accounting for only brittle and dyke lineaments (removing fabric-concordant).

4.2 Azimuth

Figure 16 shows a rose diagram of the entire integrated lineament data set, including all 4701 inferred structure types (brittle, fabric-concordant and dyke), which can be subdivided into two broad azimuth trends. The NE trending peak has a mean azimuth of 38° and the SE trending peak has a mean azimuth of 130°.

Figure 17 further subdivides the integrated lineaments and shows rose diagrams of the lineament orientations based on inferred type (i.e. brittle, fabric-concordant, dyke). Similar to the entire integrated lineament rose diagram, the brittle lineaments display a dominant NE trending peak (Figure 17A). However, the NW trending lineaments display a wider range of azimuths around the mean trend. The fabric-concordant lineaments display a pronounced SE trend, comprising of 649 lineaments with a mean azimuth of 127° and also display two subordinate sets; N and NE trends as a result of these lineaments following the variation in the ductile fabric around the northwestern edge of the Revell Batholith. The N trending set consists of 174 lineaments and has a mean azimuth of 171° and the NE trending set consists of 200 lineaments with a mean azimuth of 47°. Based on this rose diagram (Figure 17b), and the spatial distribution of fabric-concordant lineaments, these lineaments could be subdivided into three lithostructural domains and characterized by unique azimuth statistics. Future studies may evaluate these fabric-concordant structures with ductile fabric geometries (e.g. foliation, gneissic layering, etc) mapped throughout the greenstone belt (e.g. Satterly, 1960, Kresz et al 1982, Stone et al 2011a, Stone et al 2011b) to better predict their projection into the subsurface.

Figure 17c also presents a rose diagram of the dominant dyke trends. Although the rose diagram for the inferred dykes only comprise 10 lineaments, their azimuths are fairly consistent resulting in a mean azimuth of 110°. Alternatively, these dyke lineaments could be subdivided into two discrete sets with peaks at 101° and 119°, separated by a small angle. Based on dyke lineaments shown in Figure 13, the peak trending 101° tends to comprise short lineaments that appear as en-echelon segments that are linking the longer dykes that comprise the peak trending 119°.

The brittle lineaments are further evaluated in Figure 18 to show how the dominant peak azimuths change when considering their lengths. The frequency of brittle lineament azimuths shown in Figure 18A displays two broad peaks trending towards the NE and NW. By assigning the longer lineaments a higher frequency weighting, several discrete peaks become more pronounced in the rose diagram (Figure 18B), and suggests that longer lineaments may have more well-defined azimuth trends. In addition, by only analyzing lineaments with lengths greater than 500 m, Figure 18C shows peaks in the rose diagram that are further highlighted, resulting in 5 well-defined trends (N, NE, ENE, ESE, SE).

4.3 Lineament Coincidence

The integrated lineament data set results represent a combined analysis of the magnetic and surficial (LiDAR and orthoimagery) lineaments, and are believed to reflect the most accurate lineament traces from the source data. The combined analysis also resulted in the evaluation of trace lineaments that were interpreted from more than one data set (described in Section 2.2.2). Lineament coincidence analysis resulted in a total of 113 (2.4%) lineaments that were observed in both the magnetic and the surficial (LiDAR and orthoimagery) data sets (Figure 19). Their lengths ranged from 433 to 13470 m, with a median of 2591 m and a mean of 3436 m. Although these coincident lineaments only account for 2.4% of the total number of lineament, the sum of their lengths account for just over 20% of the total sum of lineament lengths. Based on these results, the coincident lineaments tend to be relatively long. Of the remaining lineaments, 4501

are only interpreted based on the LiDAR and orthoimagery data, and 88 lineaments are only interpreted from the magnetic data (Figure 19).

5. CONCLUSIONS

Performing a structural lineament interpretation is an important component of the assessment of a crystalline bedrock setting, where the interpreted lineaments have the potential to represent the surface expression of faults and fractures that may act as potential groundwater flow pathways, zones of geomechanical instability or potential reactivation. Previous lineament interpretations in the Ignace area were completed at maximum scale of 1:25,000. Since the Revell Site was selected as the area for initial borehole drilling, an updated interpretation of lineaments was completed at a closer scale.

This report documents the specific data sources, workflow, and results from an updated lineament interpretation for the Revell Batholith and surrounding greenstone belt areas. The lineament interpretation is based on high-resolution remote sensing data sets, including a high-resolution airborne magnetic data, high-resolution surface topographic data and digital orthoimagery data collected during the airborne LIDAR survey. The updated lineament analysis provides an interpretation of the location and orientation of possible brittle and dyke lineaments, as well as fabric-concordant lineaments interpreted within the greenstone belt units.

Within the Revell Batholith and surrounding greenstone belt area, a total of 192 magnetic lineaments, and 4676 surficial lineaments were interpreted to from their respective data sets. The integration of magnetic and surficial lineaments for the Revell Batholith area resulted in a total of 4701 lineament traces. As a result, the integrated lineaments comprise 3668 lineaments interpreted as brittle structures, 1023 lineaments interpreted as fabric-concordant structures, and 10 lineaments that are interpreted as diabase dykes.

The integrated lineament data set results represent a combined analysis of the magnetic and surficial lineaments, and are believed to reflect the most accurate lineament traces from the source data. Lineament coincidence analysis resulted in a total of 113 (2.4%) lineaments that were observed in both the magnetic and the surficial data sets. The lack of coincidence between magnetic and surficial lineaments could be attributed to multiple variables, including features identified in the surficial data may not possess sufficient magnetic susceptibility contrast to be recognized in the magnetic data, and masking of surface expressions of magnetic lineaments by the presence of overburden.

Evaluating lineament lengths of the final integrated lineaments resulted in lengths ranging from 17 to 13470 m, with a median length of 193 m and mean length of 402 m. Statistical descriptors were calculated that describe the fit of the lineament lengths to both lognormal and power law distributions. Although lineament lengths fit well to the lognormal distribution, calculated skewness coefficients suggest the data has a slight positive skew. In addition, cumulative frequency of lineament lengths fit the power law curve over the portion of data where measured lengths are not influenced by sampling bias effects, however deviate from the curve as a result of censoring and truncation.

Azimuth analysis of the entire integrated lineament data set, including all 4701 inferred structure types (brittle, fabric-concordant and dyke), are subdivided into a NE trending peak with a mean azimuth of 38° and a SE trending peak with a mean azimuth of 130°. The fabric-concordant lineaments display a pronounced SE trend, comprising of 649 lineaments with a mean azimuth of 127° and also display two subordinate sets; N and NE trends as a result of these lineaments following the variation in the ductile fabric around the northwestern edge of the Revell Batholith. Results suggest that the spatial distribution of fabric-concordant lineaments could be subdivided into three structural domains and characterized by unique azimuth statistics. Ten dyke lineaments show fairly consistent trends resulting in a mean azimuth of 110°. Alternatively,

these dyke lineaments could be subdivided into two discrete sets with peaks at 101° and 119°, separated by a small angle, where the peak trending 101° tends to comprise short en-echelon segments linking the longer dykes that comprise the peak trending 119°. Within the Revell Batholith, five 5 well-defined brittle lineament trends (N, NE, ENE, ESE, SE) are identified when analyzing lineaments with lengths greater than 500 m.

Overall, the process of interpreting lineaments from remotely sensed data inherently has varying degrees of uncertainty. Uncertainty can be associated with location accuracy of a given lineament trace, which can depend on the discreteness and continuity of the feature identified in a source data set. Uncertainty may be associated with the nature and extent of overburden coverage that may mask the bedrock surface, resulting in poor lineament identification from surficial datasets. Also, uncertainty may also be associated with a poor magnetic contrasts between the rock mass and potential fracture zones, which can limit the interpretation of lineaments from airborne magnetic survey data. Ultimately, the greatest uncertainty is whether the interpreted lineaments actually represent the surface expression of structures that project into the subsurface, or whether or not they are hydraulically conductive. Ultimately, these uncertainties and others should be managed through additional surface geological mapping and borehole drilling, where specific lineaments can be further characterized and their uncertainties reduced.

Results from this updated structural lineament interpretation will contribute towards a further understanding of the structural framework of the Revell Batholith and surrounding greenstone belt area. As such, the resulting lineament data sets will provide the initial framework for construction of multiple discrete fracture networks (DFN), and subsequently form the input in to groundwater flow scenarios for the area.

6. REFERENCES

ATLIS 2018. Ignace Revell Batholith LIDAR and orthoimagery survey, Ontario.

Bour, O. and Davy, P., 1997. Connectivity of random fault networks following a power law fault length distribution. Water Resources Research, 33(7), pp.1567-1583.

Golder (Golder Associates Ltd.), 2013. Phase 1 Desktop Geoscientific Preliminary Assessment of Potential Suitability for Siting a Deep Geological Repository for Canada's Used Nuclear Fuel, Township of Ignace, Ontario. Prepared for Nuclear Waste Management Organization (NWMO). NWMO Report APM-REP-06144-0011. Mississauga, Canada.

Golder (Golder Associates Ltd.) and PGW (Paterson, Grant, and Watson), 2017. Phase 2 Geoscientific Preliminary Assessment, Geological Mapping, Township of Ignace and Area, Ontario. Prepared for Nuclear Waste Management Organization (NWMO). NWMO Report APM-REP-01332-0225. Mississauga, Canada.

JDMA (J.D. Mollard and Associates Ltd.), 2013b. Phase 1 Geoscientific Desktop Preliminary Assessment, Lineament Interpretation, Township of Ignace, Ontario. Prepared for Nuclear Waste Management Organization (NWMO). NWMO Report Number: APM-REP-06144-0014.

Kresz, D., Blackburn C.E. and Fraser, F.B. 1982. Precambrian Geology of the Kewashegamuk Lake, Eastern Part. Kenora District, Ontario Geological Survey, Map P2570. Geological Series-Preliminary Map, Scale 1:15,840.

Mardia, K.V. 1972. Probability and mathematical statistics: statistics of directional data. London: Academic.

OGS (Ontario Geological Survey). 2011a. Ontario airborne geophysical surveys, magnetic and electromagnetic data, Stormy Lake area, Geophysical Data Set 1107 - Revision 1.

OGS (Ontario Geological Survey), 2011b. 1:250 000 scale bedrock geology of Ontario, Miscellaneous Release Data 126 - Revision 1.

Pickering, G., Bull, J.M. and Sanderson, D.J. 1995. Sampling power-law distributions. Tectonophysics, 248(1-2), pp.1-20.

PGW (Patterson, Grant and Watson Ltd.), 2013. Phase 1 Geoscientific Desktop Preliminary Assessment, Processing and Interpretation of Geophysical Data, Township of Ignace, Ontario. Prepared for Nuclear Waste Management Organization (NWMO). NWMO Report APM-REP-06144-0013.

QGIS, 2017. QGIS geographic information System. V 2.18. Open source geospatial Foundation project.

Satterly, J. 1960. Dyment area, District of Kenora, Ontario; Ontario Department of Mines, Map 1960H, 1:31 680.

SGL (Sander Geophysics Ltd.), 2015. Phase 2 Geoscientific Preliminary Assessment, Acquisition, Processing and Interpretation of High-Resolution Airborne Geophysical

Data, Township of Ignace, Ontario. Prepared for Nuclear Waste Management Organization (NWMO). NWMO Report APM-REP-06145- 0002. Toronto, Canada.

SRK (SRK Consulting Inc.), 2015. Phase 2 Geoscientific Preliminary Assessment, Lineament Interpretation, Township of Ignace, Ontario. Prepared for Nuclear Waste Management Organization (NWMO). NWMO Report APM-REP-06145-0003. Toronto, Canada.

SRK (SRK Consulting Inc.) and Golder (Golder Associates Ltd.), 2015. Phase 2 Geoscientific Preliminary Assessment, Observation of General Geological Features, Township of Ignace, Ontario. Prepared for Nuclear Waste Management Organization (NWMO). NWMO Report APM-REP-06145-0004. Toronto, Canada.

Stone, D., B. Hellebrandt and M. Lange, 2011a. Precambrian Geology of the Bending Lake Area (South Sheet). Ontario Geological Survey, Preliminary Map P.3623, Scale 1:20 000. Sudbury, Canada.

Stone, D., B. Hellebrandt and M. Lange, 2011b. Precambrian Geology of the Bending Lake Area (South Sheet). Ontario Geological Survey, Preliminary Map P.3624, Scale 1:20 000. Sudbury, Canada

Thommeret, N., J. S. Bailly, and C. Puech. "Robust extraction of Thalwegs networks from DTMs for topological characterisation: a case study on badlands." Proceedings of Geomorphometry 31 (2009): 218-223.

Yokoyama, R., Shirasawa, M., Pike, R.J. 2002. Visualizing topography by openness: A new application of image processing to digital elevation models. Photogrammetric Engineering and Remote Sensing, Vol.68, pp.251-266

FIGURES

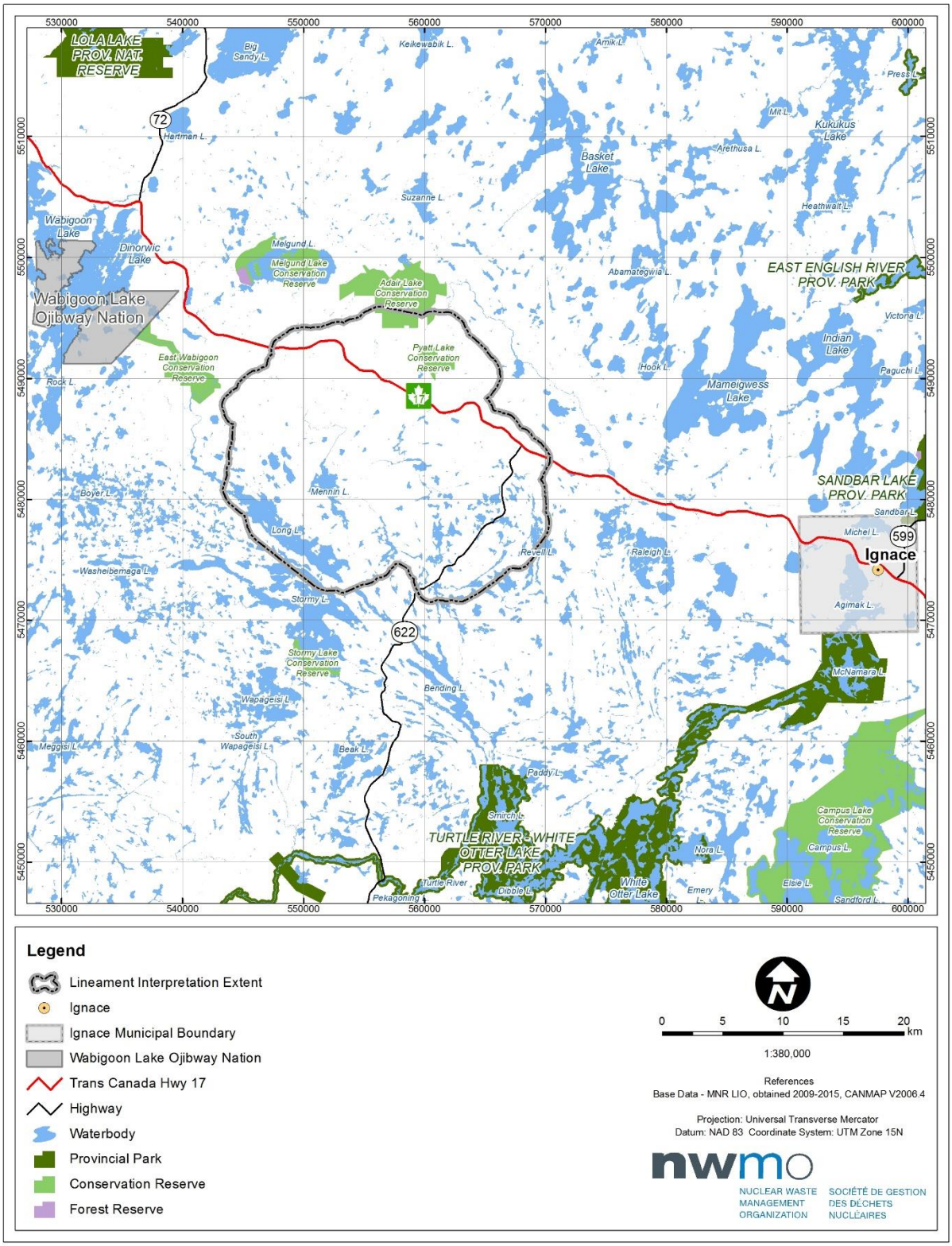

Figure 1. Location of lineament interpretation extent within Northwestern Ontario.

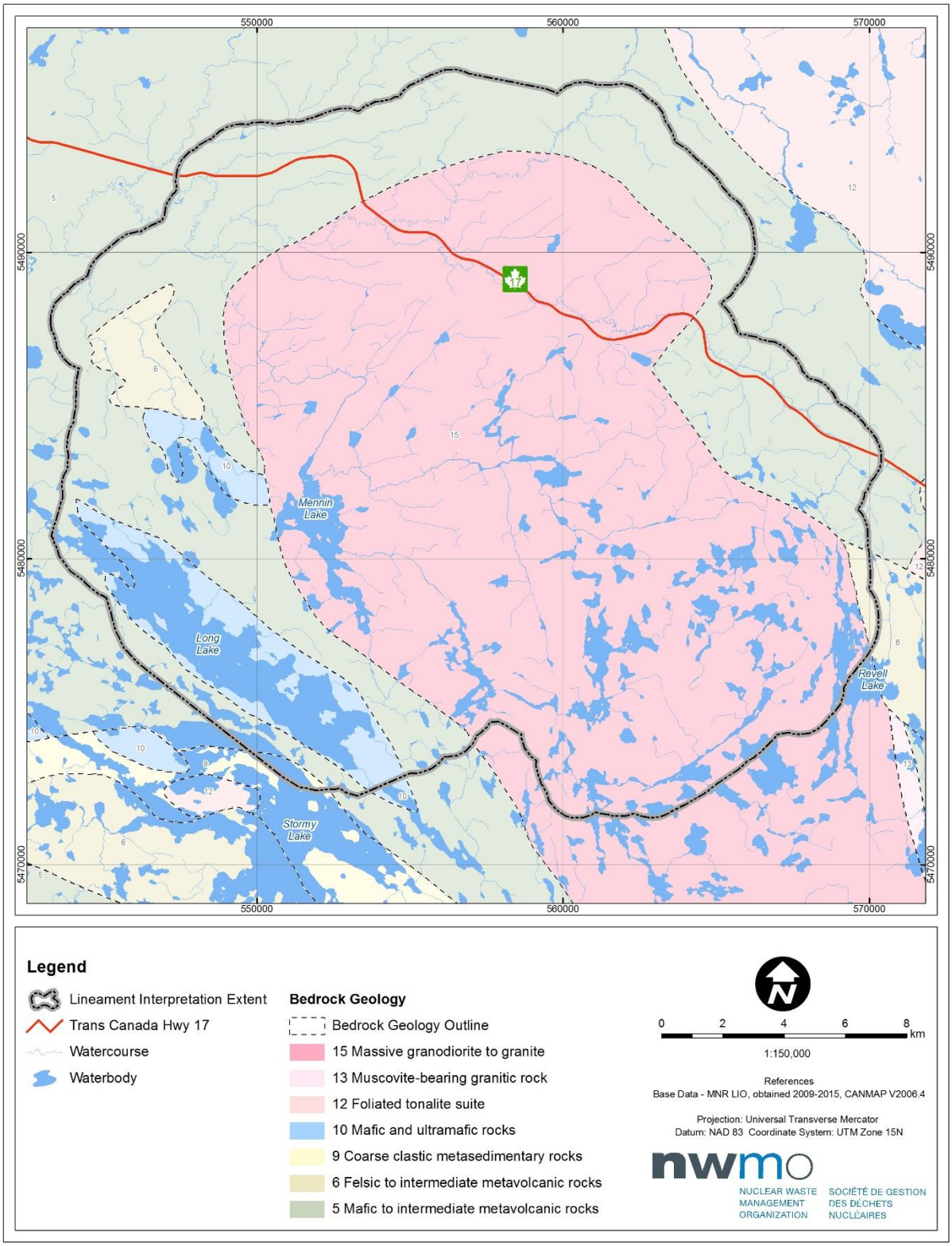

Figure 2. Bedrock Geology in the area around the Lineament Interpretation Extent. Bedrock geology presented is the 1:250,000 scale regional geology from the Ontario Geological Survey (MRD126-r1: OGS 2011b)

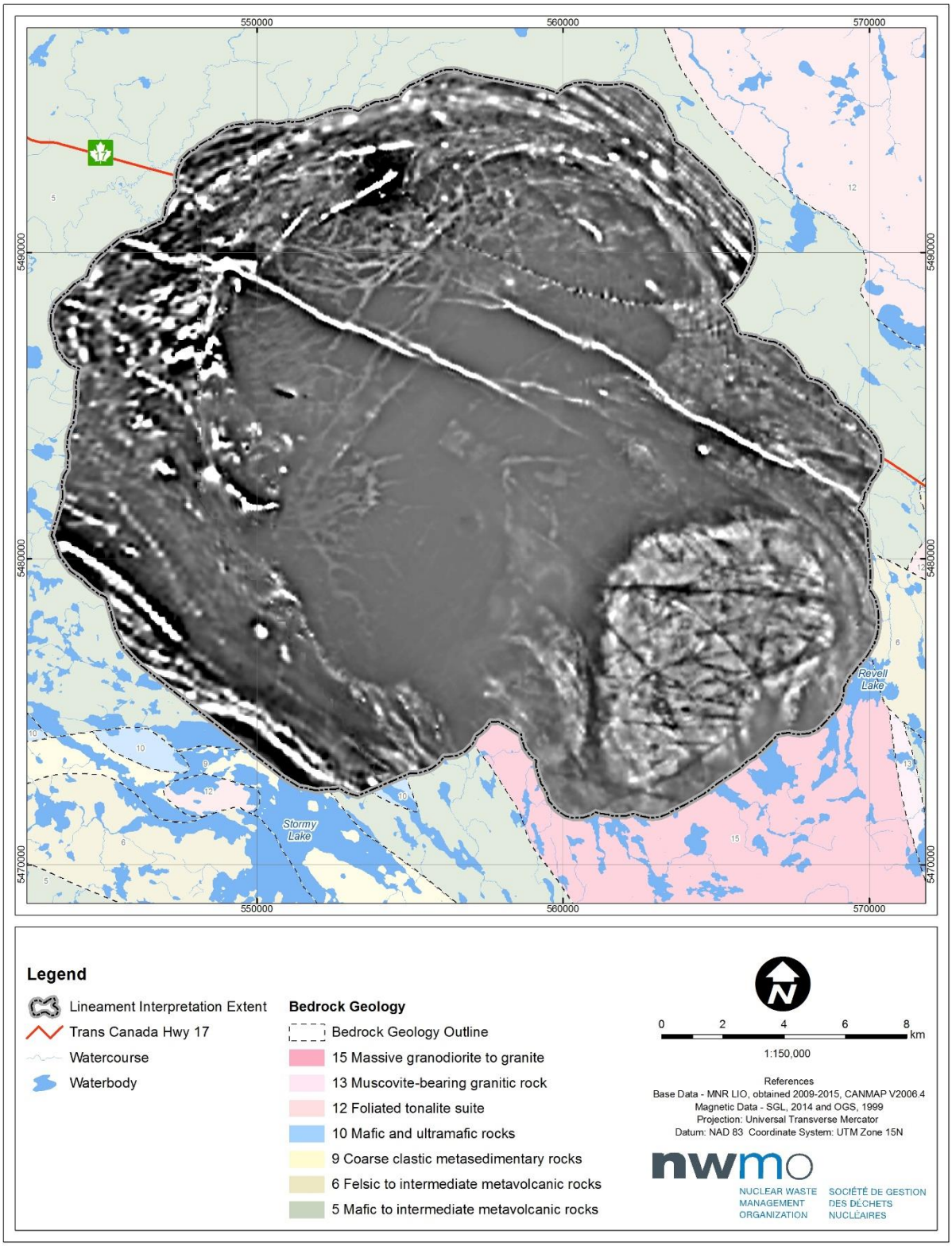

Figure 3. First vertical derivative of the total magnetic field data acquired by Sander Geophysics Limited (SGL 2015), supplemented by magnetic data from the OGS 2011a along the western portion of the area.

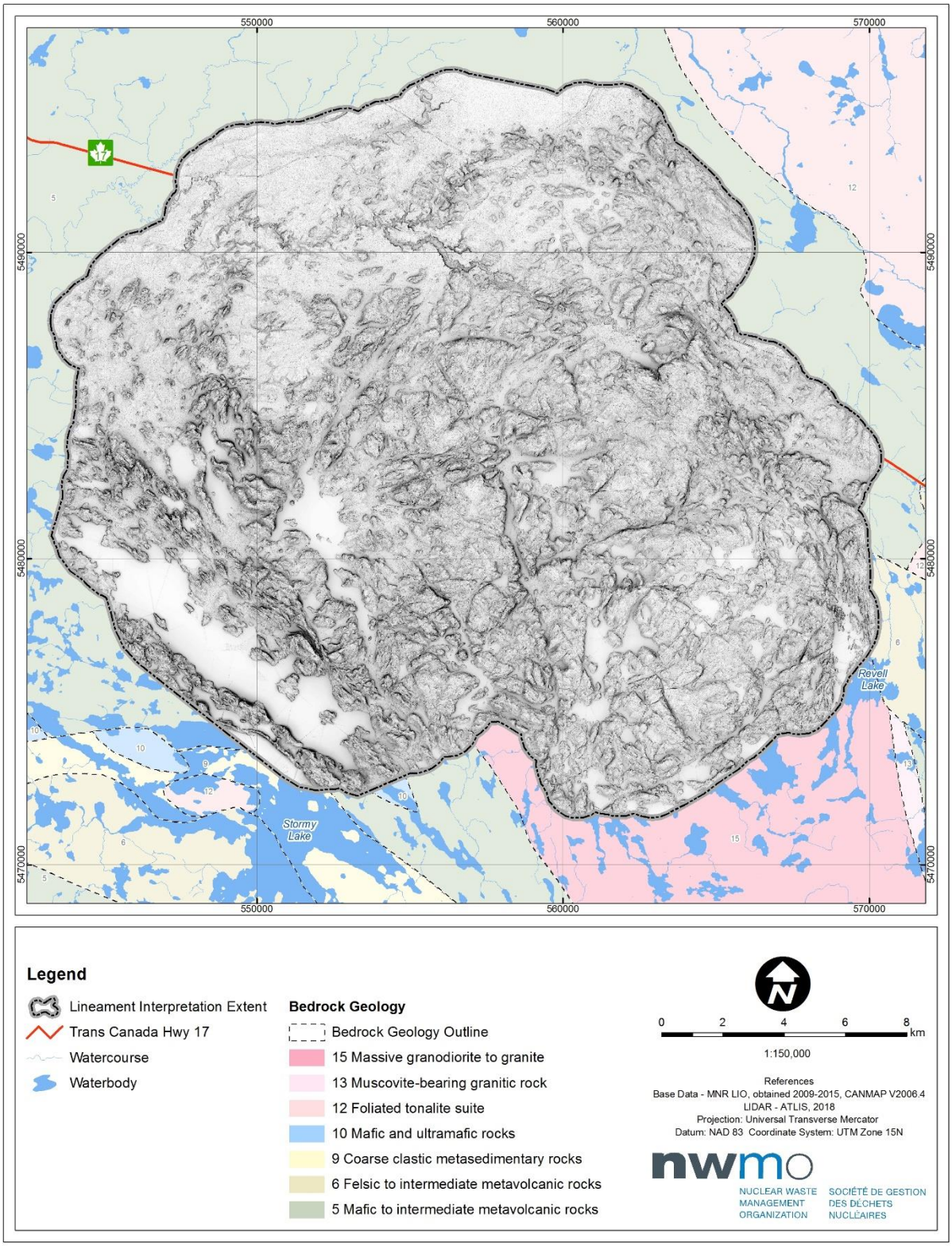

Figure 4. Terrain positive openness grid derived using the digital elevation data from aerial LiDAR survey acquired by ATLIS Geomatics (ATLIS 2018).

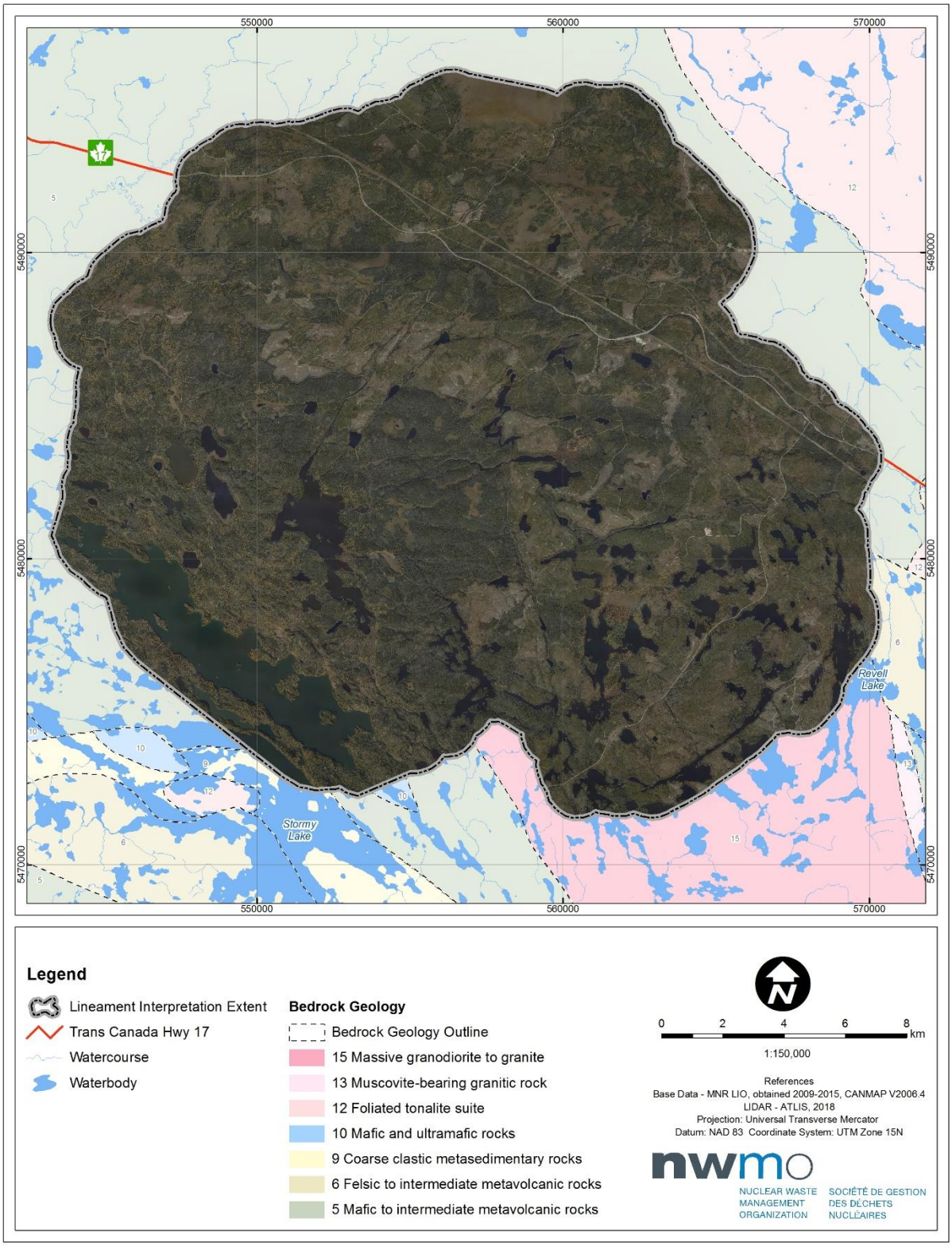

Figure 5. RBG true colour orthoimagery mosaic acquired by ATLIS Geomatics in Fall 2017 (ATLIS 2018).

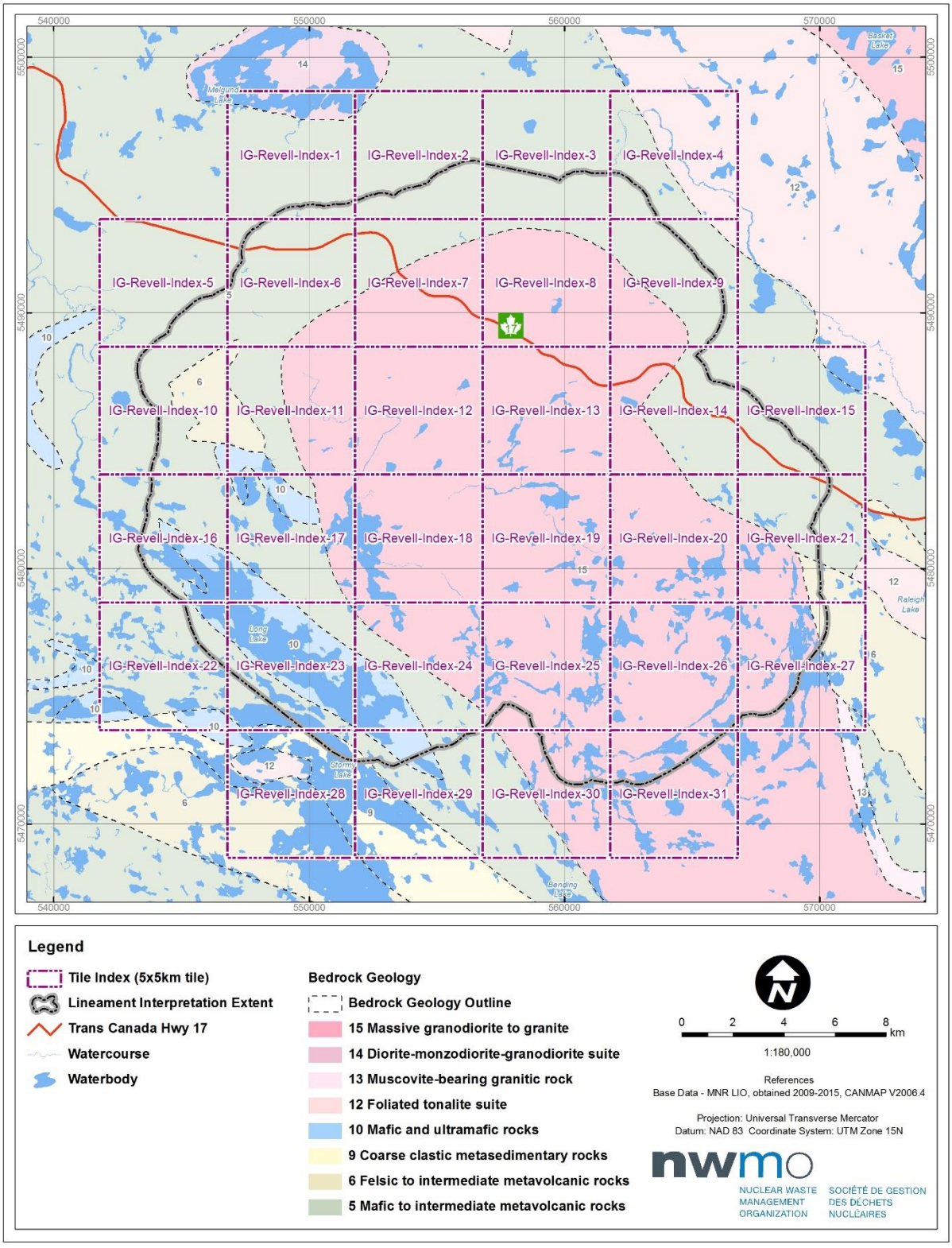

Figure 6. Lineament interpretation extent and a tile index (i.e. 5 x 5 km tiles) to be used during a systematic lineament workflow.

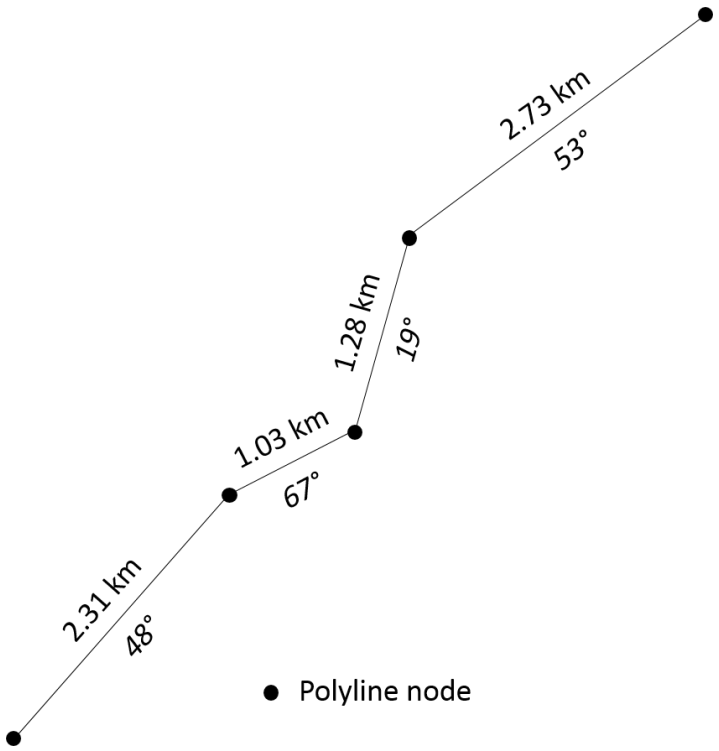

Figure 7. Schematic of lineament trace made up of four polyline segments and 5 nodes. Each polyline segment can be characterized by its length and azimuth from its start and end nodes.

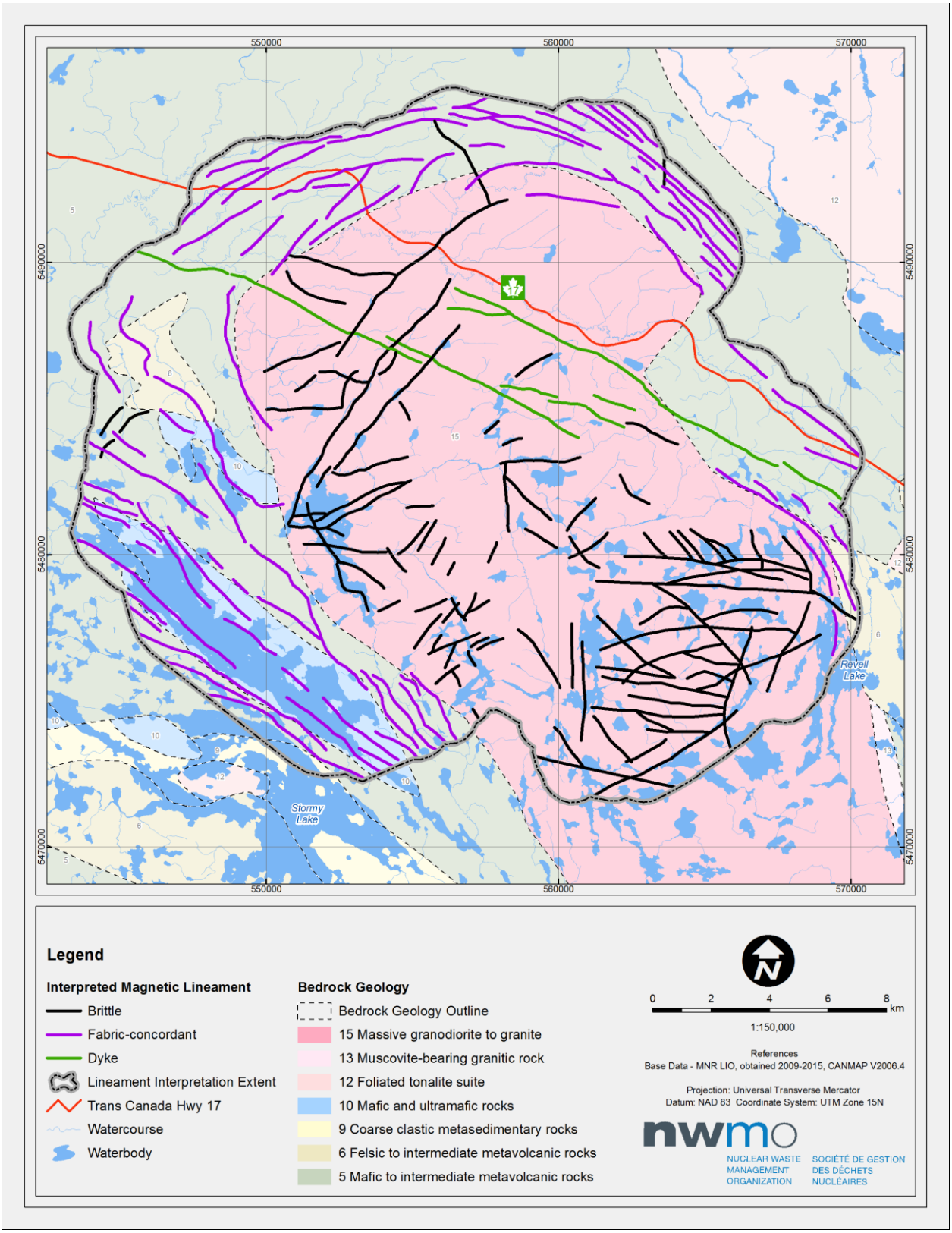

Figure 8. Interpreted magnetic lineaments within the Revell Batholith and surrounding greenstone belt area. Purple lines represent fabric-concordant lineaments, and are concordant with planar ductile fabric in the metavolcanic and metasedimentary rocks of the greenstone belts. Green lines represent diabase dykes. Black lines represent brittle lineament structures. Lineaments are overlain on bedrock geology.

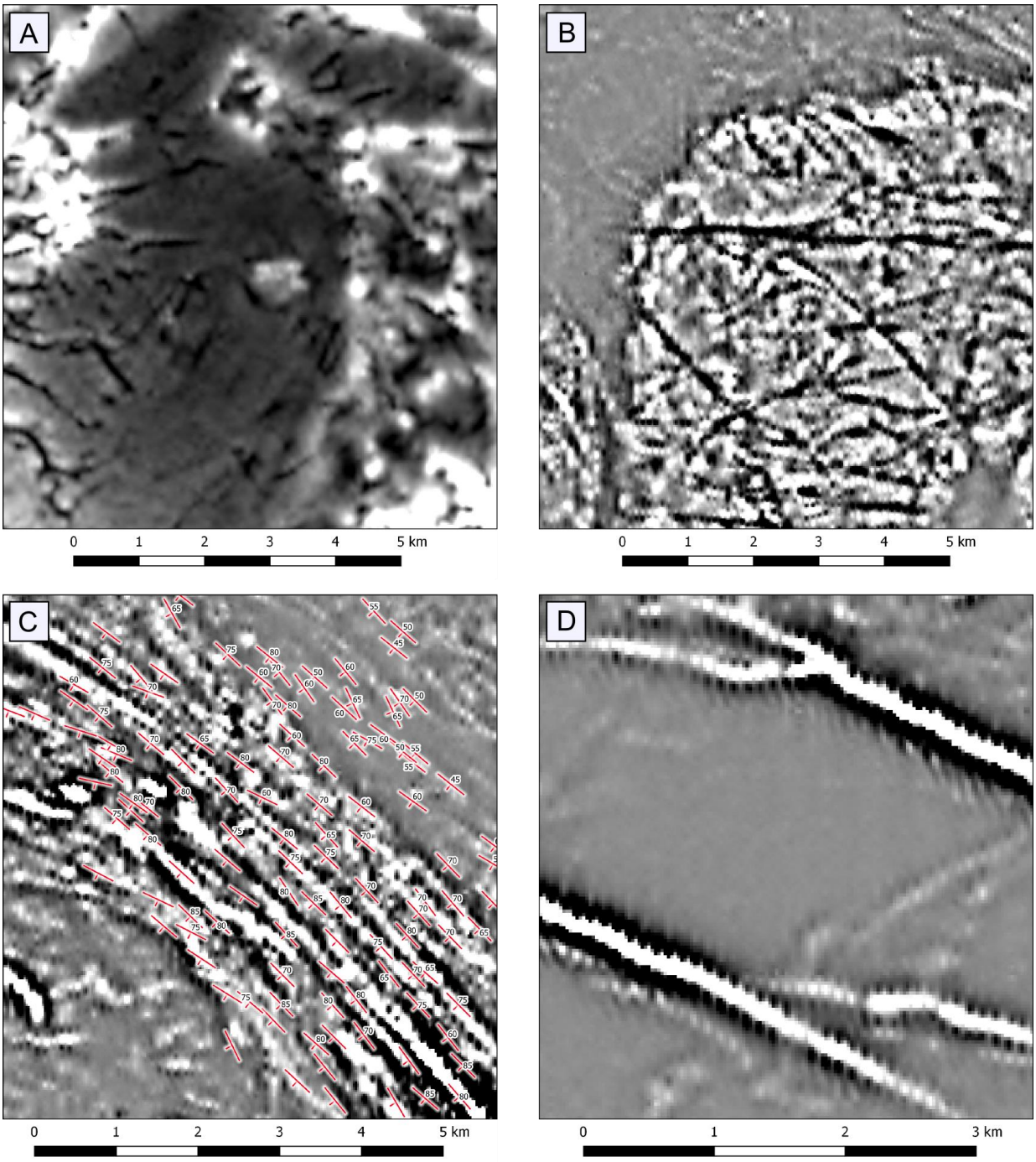

Figure 9. Examples of magnetic source data expression used to trace magnetic lineaments. (A) several linear low magnetic anomalies inferred to be brittle lineaments within the Revell Batholith in the total magnetic gradient data, (B) strong linear magnetic anomalies inferred to be brittle lineaments within the megacrystic phase of the Revell Batholith, (C) strong NW trending magnetic fabric that is concordant with mapped foliation and schistosity trends (Satterly, 1960, Kresz et al 1982, Stone et al 2011a, Stone et al 2011b), and (D) NW trending high magnetic anomalies cutting through the Revell Batholith interpreted as diabase dykes.

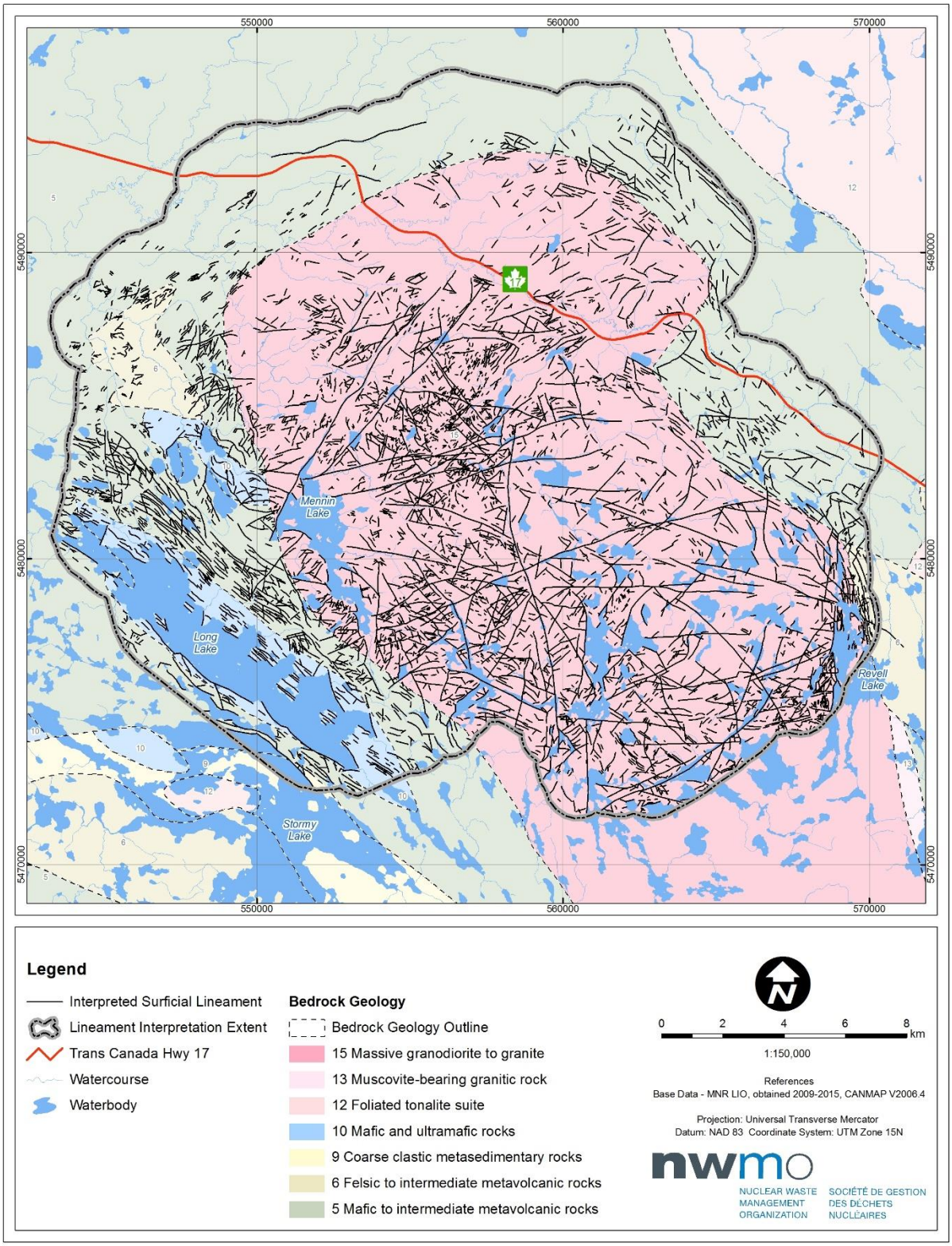

Figure 10. Interpreted surficial lineaments, derived from LiDAR and orthoimagery data, within the Revell Batholith and surrounding greenstone belt area.

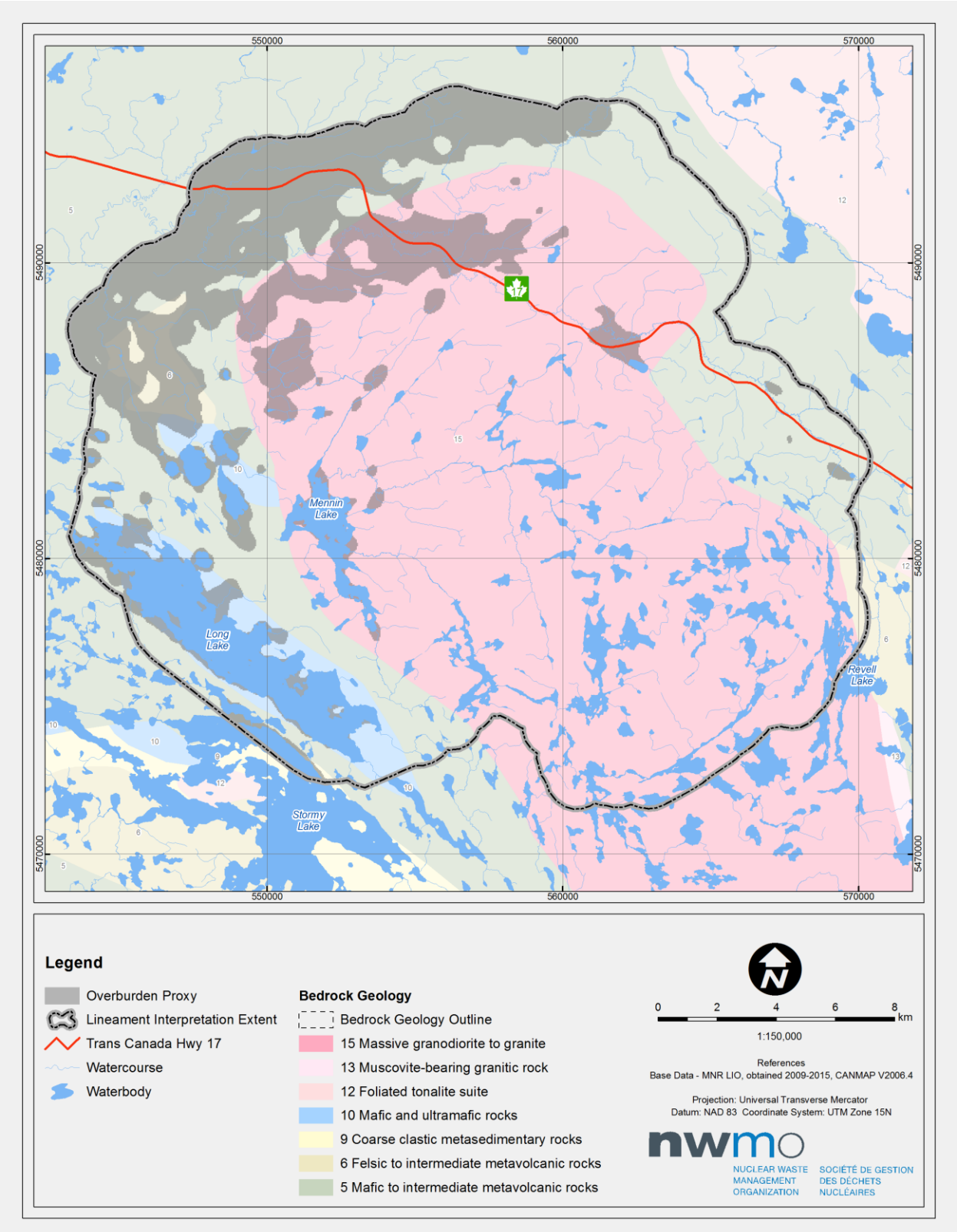

Figure 11. Distribution of inferred overburden (grey), based on airborne electromagnetic conductance grid and large water bodies.

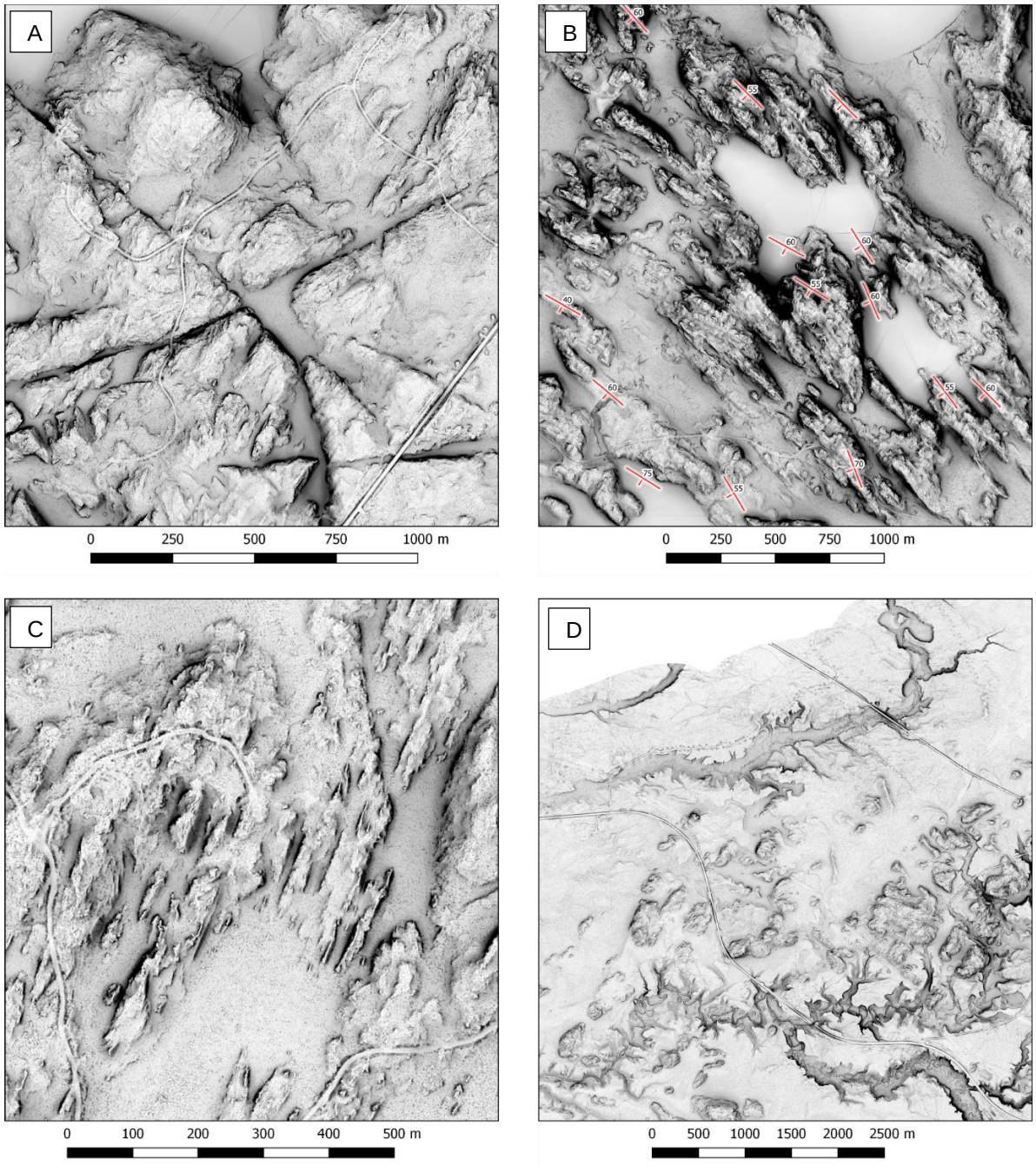

Figure 12. Examples of expressions in the LiDAR source data used to trace surficial lineaments. (A) several discrete linear topographic valleys within the Revell Batholith shown from the LiDAR data, (B) strong NW trending linear valleys and scarp faces that is concordant with mapped foliation and schistosity trends within the greenstone belt units (Satterly, 1960, Kresz et al 1982, Stone et al 2011a, Stone et al 2011b), (C) NE trending short and discontinuous, linear valleys within the Revell Batholith, and (D) area of significant overburden characterized by low topographic relief, and numerous meandering river valleys in the northern portion of the lineament assessment area.

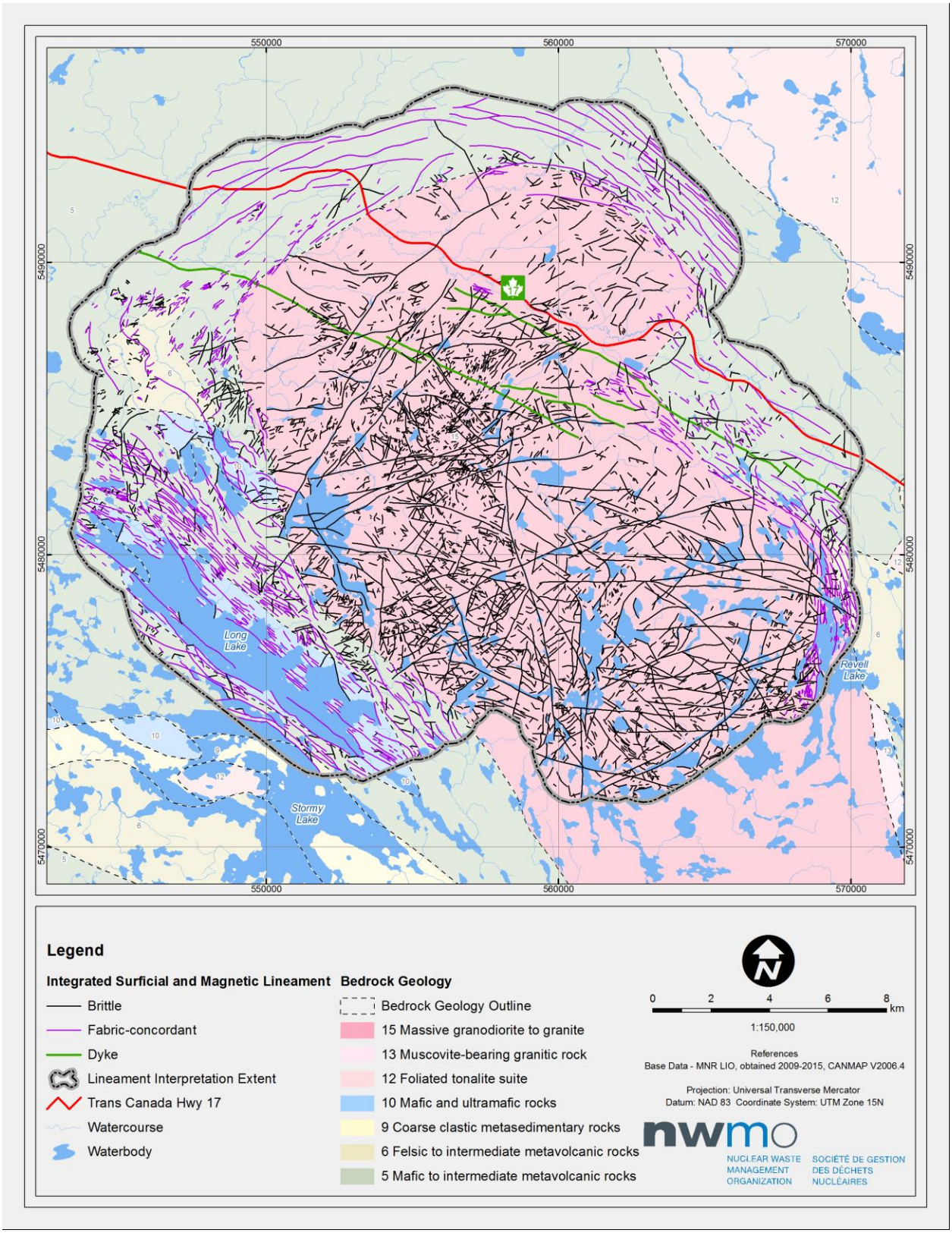

Figure 13. Integrated surficial and magnetic lineaments within the Revell Batholith and surrounding greenstone belt area. Purple lines represent fabric-concordant, and are concordant with ductile fabric in the metavolcanic and metasedimentary rocks of the greenstone belts. Green lines represent diabase dykes. Black lines represent brittle lineament structures. Lineaments are overlain on bedrock geology.

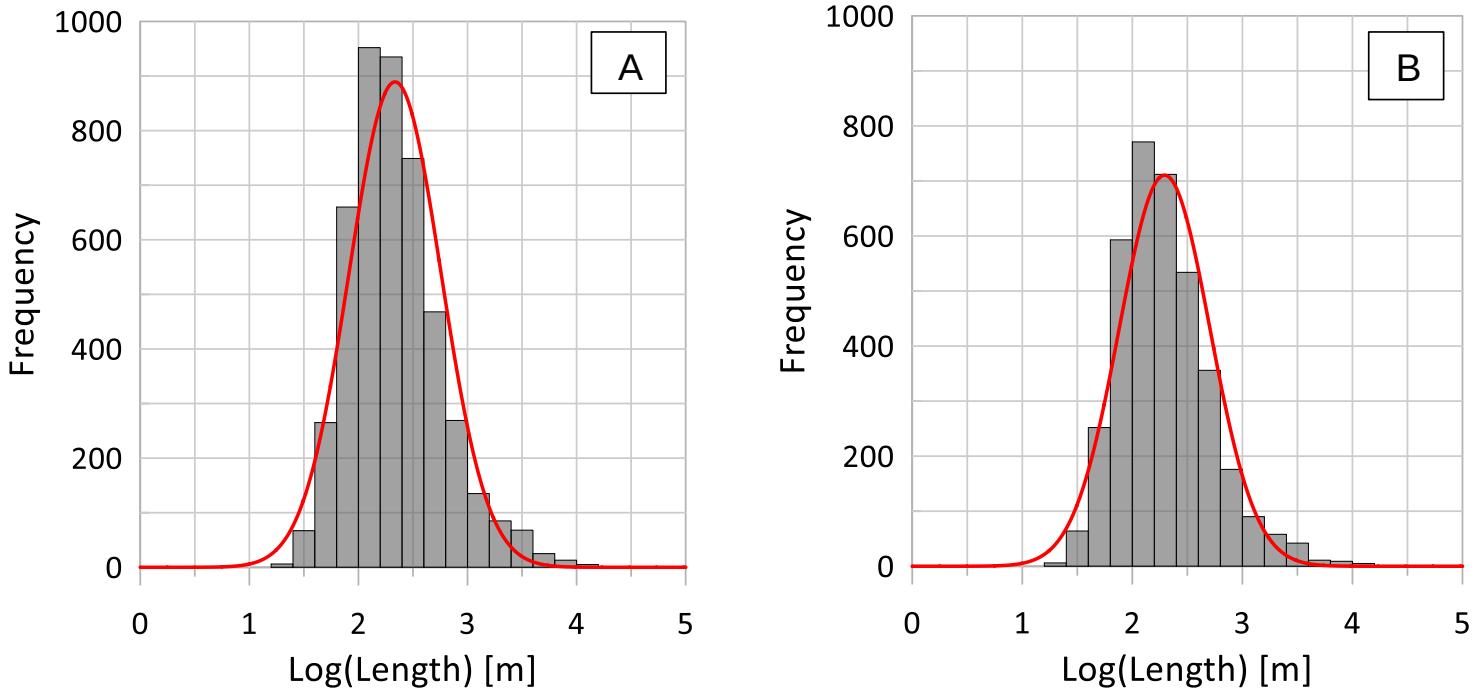

Figure 14. Histogram of logarithmic lengths [m] for (A) all integrated lineament, and (B) inferred brittle and dyke lineaments. The red line shows a lognormal distribution model.

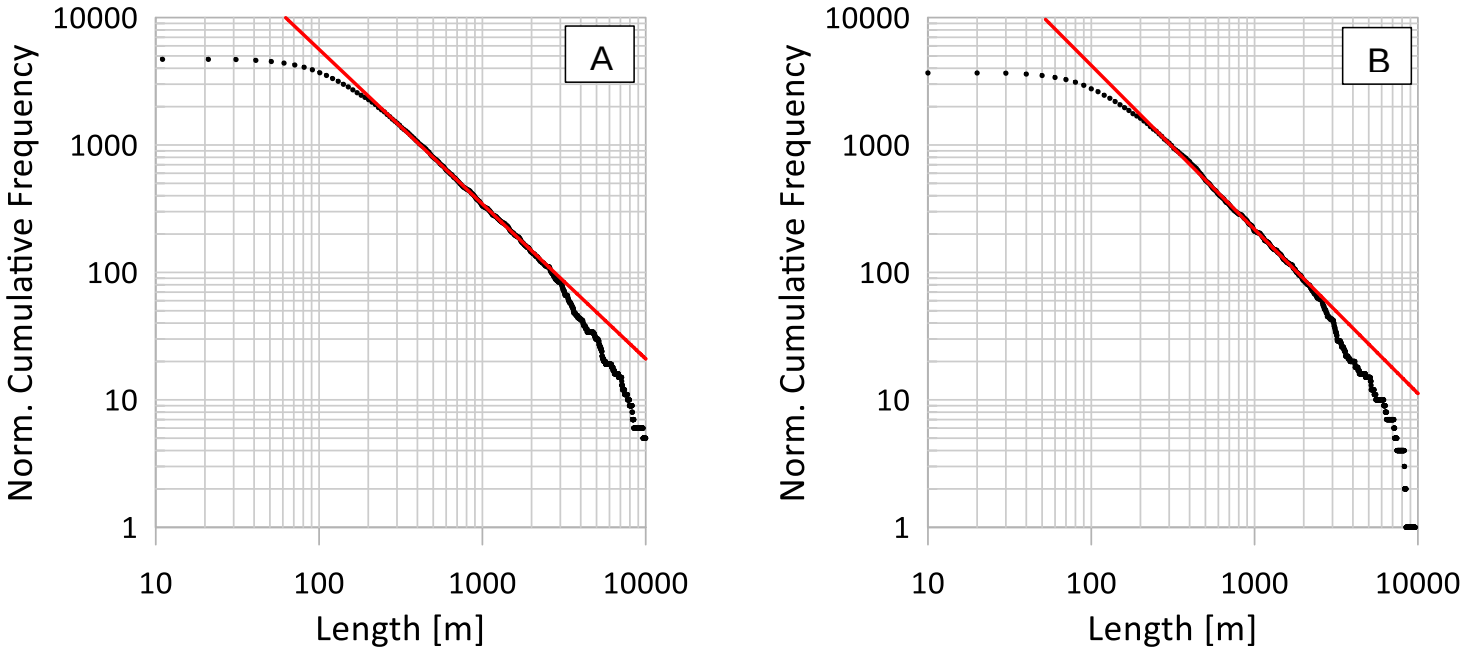

Figure 15. Power law fit through the normalized cumulative frequency distributions of lineament lengths for (A) all integrated lineaments and (B) inferred brittle and dyke lineaments. The normalized cumulative frequency distributions represent the number of lineaments (y axis) that exceed a given length (x axis). Power law curves (red line) are fit to the data between the apparent censoring and truncation points.

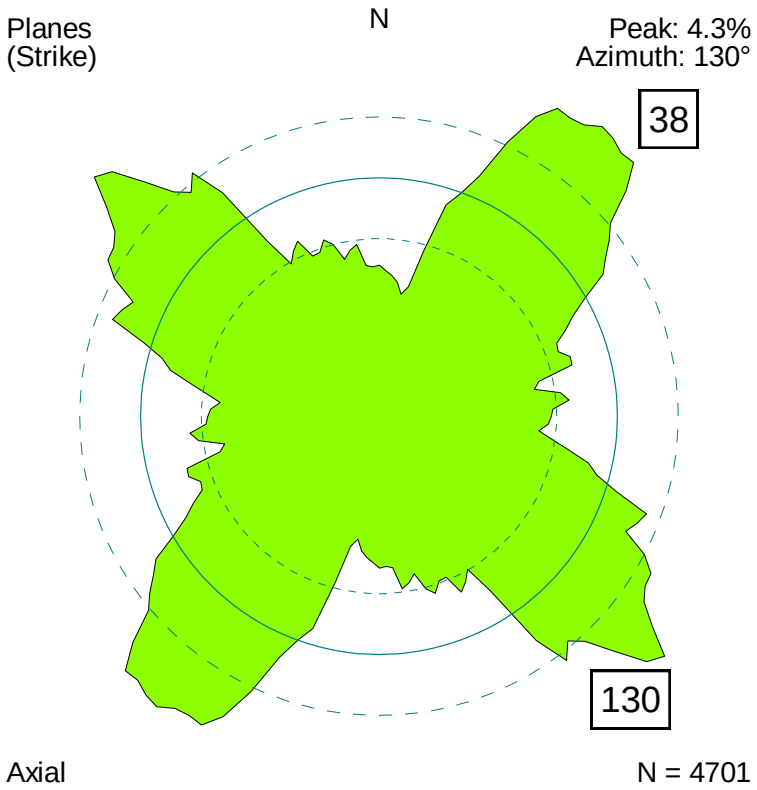

Figure 16. Rose diagram of all integrated lineament data set. Lineament frequencies are counted based on 5° bins.

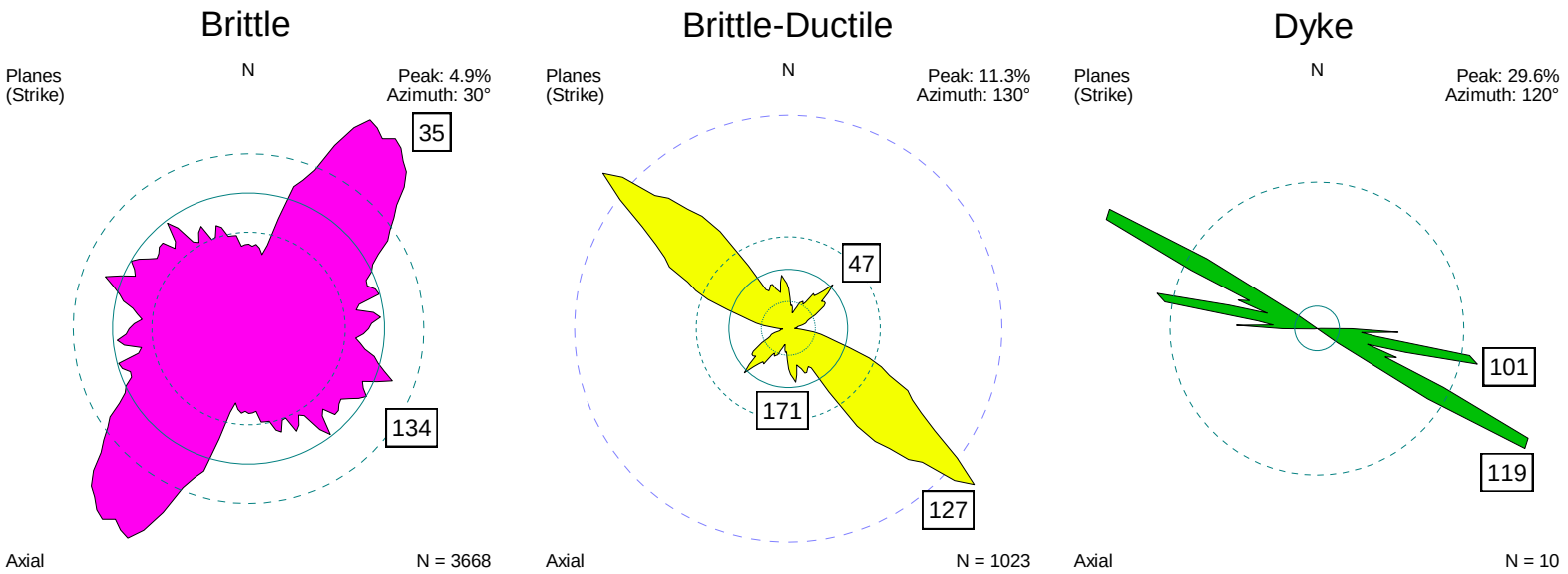

Figure 17. Rose diagrams subdivided based on inferred lineament type showing brittle, fabric-concordant, and dykes. Lineament frequencies are counted based on 5° bins. 'N' represents the number of data points used.

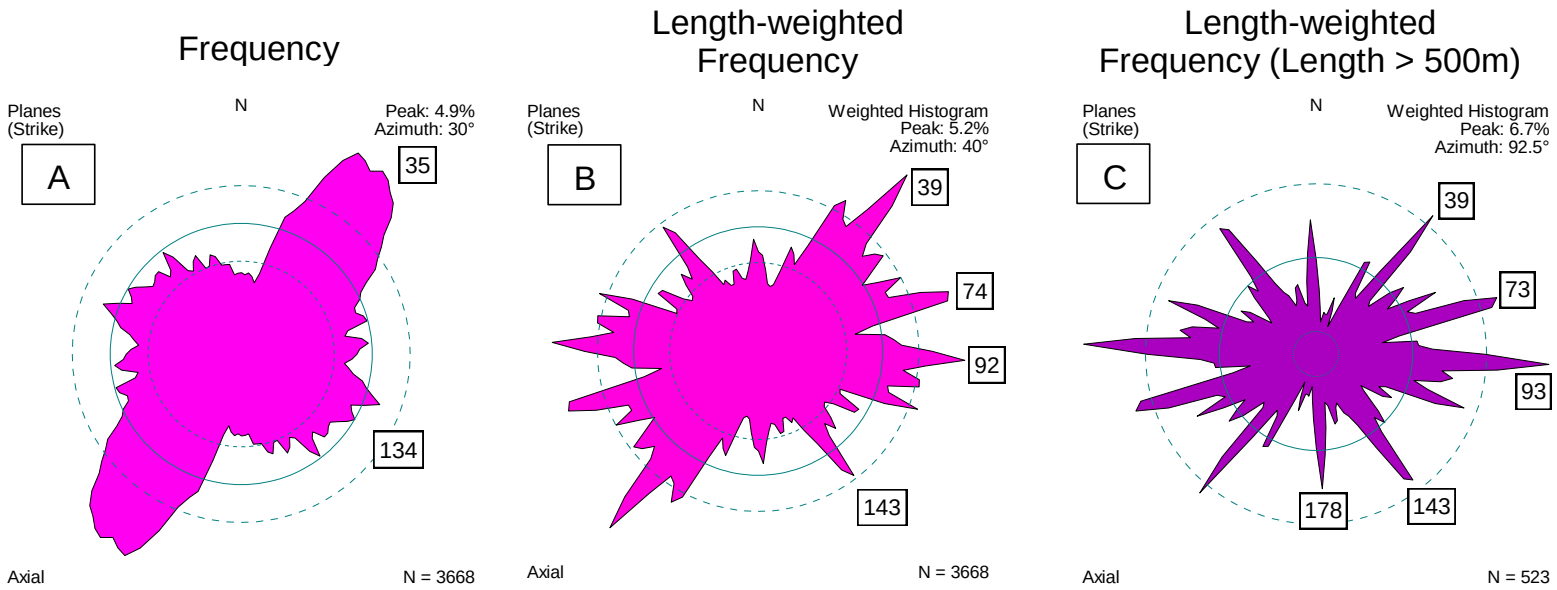

Figure 18. Brittle lineament rose diagrams showing (A) frequency, (B) length-weighted frequency, and (C) length-weighted frequency of lineaments greater than 500 m. Lineament frequencies are counted based on 5° bins.

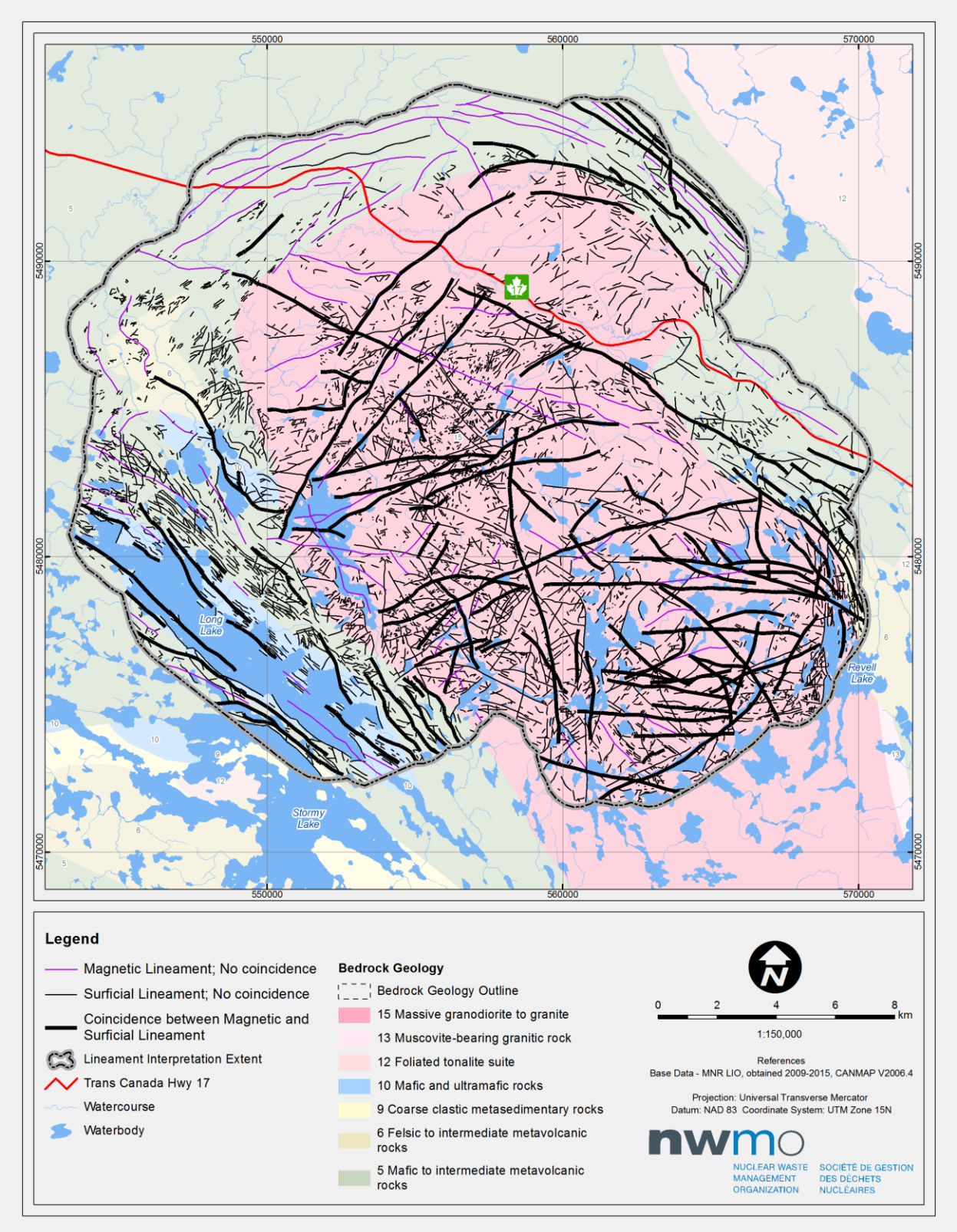

Figure 19. Spatial distribution of interpreted lineaments with and without coincidence between data sets. Bold black lines represent lineaments coinciding between magnetic and surficial lineaments. Thin purple (magnetic) and thin black (surficial) lines represent lineaments with no coincidence between data sets.